

ADOPTIVE TRANSFER STUDIES TO ESTABLISH A
MODEL OF PHASE II EXOCRINE GLAND DYSFUNCTION IN THE NOD MODEL
OF SJÖGREN'S SYNDROME

By

VINETTE B. BROWN

A THESIS PRESENTED TO THE GRADUATE SCHOOL
OF THE UNIVERSITY OF FLORIDA IN PARTIAL FULFILLMENT
OF THE REQUIREMENTS FOR THE DEGREE OF
MASTER OF SCIENCE

UNIVERSITY OF FLORIDA

2004

Copyright 2004

by

Vinette B. Brown

This document is dedicated to the graduate students of the University of Florida.

ACKNOWLEDGMENTS

Working on this project has been a wonderful experience. As a master's student I had the opportunity to learn from very knowledgeable professors and researchers. Many people assisted me in the completion of my degree, for which I am very thankful.

First and foremost, I would like to thank Dr. Ammon B. Peck who has provided a great deal of support and advice. I am so grateful to have worked under someone who is extremely knowledgeable but is also willing to listen to new ideas. I would like to thank Dr. Michael Humphreys-Beher for allowing me to enter his lab and giving me my very first project. I am very grateful for the help I received from my committee members, Dr. Sally Litherland and Dr. David Ostrov, who opened their labs and offices to me.

I would like to thank my entire lab who has provided an immense amount of support. I would like to thank Janet Cornelius and Dr. Seunghee Cha who aided me with their years of experience and lots of their time. I also thank Lori Boggs, Daniel Saban, Eric Sing-Son and Smruti Killedar who have both provided lots of technical assistance and advice.

I am very grateful for all of the support I received outside of the Peck lab. I thank Dr. Clare-Salzler's laboratory, Dr. Petersen's laboratory, Dr. Burne's laboratory, Dr. Oh's laboratory, and Dr. Khan's laboratory for all of the assistance.

I would also like to thank my friends who provided much needed moral support and a great deal of advice, specifically, Grace Kim and Dr. Kenyon Meadows.

TABLE OF CONTENTS

	<u>page</u>
LIST OF TABLES	vii
LIST OF FIGURES	viii
ABSTRACT	ix
CHAPTER	
1 INTRODUCTION	1
Background of Sjögren’s Syndrome.....	1
Animal Models	5
Adoptive Transfer Studies	13
2 MATERIALS AND METHODS	16
Animals.....	16
Adoptive Transfer.....	16
Saliva Collection.....	17
Protein Concentration	18
Amylase Activity Analysis	18
Apoptosis Detection.....	20
Apoptosis Detection via Flow Cytometry	20
Akt Expression via Polymerase Chain Reaction	22
Agarose Gel Electrophoresis	23
Caspase-3 Activity Detection	24
In Situ Apoptosis Detection Kit.	24
Detection of Infiltration	25
3 RESULTS	27
Adoptive Transfer	27
Saliva Collection.....	28
Amylase Activity Analysis	29
Amylase Activity Detected in Saliva.	29
Detection of Salivary Gland Amylase Activity	29
Protein Concentration	30
Apoptosis Detection.....	32

Apoptosis Detection via Flow Cytometry	32
Caspase-3 Activity Detection	34
Akt Expression via Polymerase Chain Reaction	34
In Situ Apoptosis Detection Kit.	36
Detection of Infiltration	36
4 DISCUSSION.....	40
LIST OF REFERENCES.....	49
BIOGRAPHICAL SKETCH	52

LIST OF TABLES

<u>Table</u>	<u>page</u>
3-1 Adoptive transfer, combinations of donor splenocytes transferred to the <i>scid</i>	28
3-2 The saliva from each adoptively transferred <i>scid</i> was collected and quantified	31
3-3 The submandibular glands for the adoptively transferred <i>scid</i> mice and the controls were collected and homogenized.....	32
3-4 Apoptosis detection using Apo-Direct kit (BD Pharmingen)	33
3-5 Akt expression ratios	35
3-6 Focus score derived from H+E stained slides of smg glands.....	39

LIST OF FIGURES

<u>Figure</u>	<u>page</u>
1-1 Apoptosis pathway. Notice that AKT is an inhibitor early in the pathway and Caspase-3 one of the last activated caspases (7).....	9
3-2 Immunohistochemical staining of submandibular glands for lymphocyte-infiltrations	37
3-3 Hematoxylin/eosin-stained tissue sections of submandibular glands	38

Abstract of Thesis Presented to the Graduate School
of the University of Florida in Partial Fulfillment of the
Requirements for the Degree of Master of Science

ADOPTIVE TRANSFER STUDIES TO ESTABLISH A
MODEL OF PHASE II EXOCRINE GLAND DYSFUNCTION IN THE NOD MODEL
OF SJÖGREN'S SYNDROME

By

Vinette B. Brown

August 2004

Chair: Ammon B. Peck
Major Department: Medical Sciences

Sjögren's Syndrome (SjS) is an autoimmune exocrinopathy that results in the development of xerostomia (dry mouth) and keratoconjunctivitis (dry eyes). There are two distinct phases of SjS. Phase I which is lymphocyte independent and phase II which is lymphocyte-dependent. The non-obese diabetic (NOD/LtJ) mouse displays symptoms associated with both phases of the disease and, therefore, is a useful model for studying SjS. The insertion of the *scid* mutation into the NOD/LtJ background has led to the development of the NOD.CB17-PrkdcScid/J (*scid*). The *scid* mouse develops phase I of SjS but as a result of the absent lymphocytes, development of phase II does not occur. The lack of mature lymphocyte development in the *scid* allows it to be used as a recipient in adoptive transfer studies to determine the combination of lymphocytes required to induce phase II of SjS.

The work described in this thesis involves the transfer of lymphocyte combinations derived from specific strains, all of which have the same NOD/LtJ genetic background, into the *scid* mouse. Adoptively transferred *scid* mice were analyzed for the progression of disease. Observation of the salivary flow, saliva proteins, presence of apoptosis and infiltration provided information on progression of disease.

Results indicate the adoptive transfer of functional lymphocytes can lead to development of phase II. However, the time required for disease progression may vary depending on the origin of the lymphocytes. The development of this adoptive transfer model has provided parameters for future experiments which may clarify the immunopathology important in progression of phase II and onset of SjS-like disease.

CHAPTER I INTRODUCTION

Many illnesses decrease the quality of life, often making normal daily tasks extremely difficult. Sjögren's syndrome (SjS) is one such disease, which often causes the patient great discomfort. Patients afflicted with SjS have difficulties eating and speaking, due to an inability to secrete saliva. These patients also have dry eyes; therefore, they have a constant feeling of irritation in the eyes. The etiology of SjS is not known and a cure is not available. The current treatment for SjS is salivary and tear stimulants (1). These stimulants are sometimes effective, providing a limited amount of relief, but they can also have undesirable side effects. By understanding the underlying causes and mechanism of SjS, a more complete treatment can be devised.

Background of Sjögren's Syndrome

In 1932, Henrik Sjögren reported the triad of keratoconjunctivitis sicca (dry eyes), xerostomia (dry mouth), and rheumatoid arthritis (2). This triad of symptoms became known as Sjögren's Syndrome, a chronic autoimmune disorder in which the secretory functions of various exocrine glands are disrupted. The major areas affected are the lacrimal and salivary glands, as well as the skin, upper respiratory, gastrointestinal tract and the genitals. The resulting dryness of mucosal surfaces results in various complications such as gastrointestinal discomfort, difficulty speaking, fatigue and musculoskeletal complaints (3). The disease is not usually fatal, but can be quite distressful for those affected. Furthermore, due to the immunological basis of the disease, patients with SjS are at an increased risk of developing a non-Hodgkin's B-cell

lymphoma. At this time, the exact etiology is not known, so patients remain uncured.

Today, patients are usually treated with secretagogues, which induce lacrimal and salivary secretion, along with other glandular secretion.

While secretagogues are readily available, a patient may not receive this treatment due to the difficulties diagnosing SjS. As with many systemic diseases, SjS appears with a wide range of clinical manifestations. These variations, may lead clinicians to misdiagnose symptoms. There are numerous reports describing lung, renal and central nervous system (CNS) involvement (4). Over the years, a number of disease classifications (San Francisco, San Diego, California, Japanese, European original and European revised), each with their own methods and standards for diagnosing Sjögren's syndrome, have been proposed. Among the different classification systems, xerostomia (dry mouth) is usually diagnosed by a lip biopsy. The demonstration of focal lymphocytic infiltrates, on a minor salivary gland (SG) biopsy, has remained the gold standard for the oral component of SjS (2). A salivary gland is considered infiltrated when there are clusters of fifty or more lymphocytes, known as foci, present. For most classification systems the presence of two foci per 4 mm² is required to identify the gland as being infiltrated. A less invasive measure of xerostomia is the use of scintigraphy and sialography. Scintigraphy is a technique where an appropriate, short-lived gamma-emitting radioisotope is introduced. Through radiographic imagery the uptake, concentration and excretion of the radioisotope by the major salivary gland (submandibular) is measured. This can be a very sensitive test for glandular function. Sialography is a similar method in which the release of saliva by the salivary glands is evaluated via [nuclear imaging](#).

Keratoconjunctivitis (dry eyes) is typically diagnosed by tear volume measured by what has become known as the Schirmer test. This test measures tear stability by the non-invasive break up time and usage of a rose bengal dye to stain the ocular surface, which results in identification of epithelial cell destruction (5). Serologic tests for the detection of autoantibodies, specifically SS-A (anti-Ro), SS-B (anti-La), and anti-nRNP, are also used for correct diagnosis of SjS. In eighty-six Sjögren's syndrome patient sera, more than 96% had SS-A, and 87% had SS-B, compared to 95% of patients with anti-nRNP (6). Serology not only facilitates diagnosis, but also can be useful in predicting the subsequent outcome and complications in patients with primary Sjögren's syndrome (2). The presence of anti-SS-A antibodies may identify patients with systemic disease (7), and in anti-SS-A/ anti-SS-B positive patients, the relative risk of developing non-Hodgkin lymphoma has been reported as high as 49.7%, within 10 years of diagnosis (4).

There are two types of Sjögren's syndrome. Individuals that exhibit the classic symptoms (dry eyes and dry mouth), in the absence of another autoimmune disease, are diagnosed as having primary SjS. Secondary SjS includes the presence of the aforementioned symptoms, in addition to another autoimmune rheumatic disease, such as rheumatoid arthritis (RA) or systemic lupus erythematosus (SLE). Due to the variability in classification systems, the exact percentage of patients with SjS is not known, but it is estimated to have a prevalence not exceeding 0.6% of the general population (2). As with most connective tissue autoimmune diseases, there is a sexual dimorphism present in Sjögren's syndrome. There is a 9:1 ratio of women to men in SjS, with most women presenting symptoms of the disease between the ages of 40 and 60 years of age.

A prominent feature of Sjögren's syndrome is the genetic predisposition (2). It is not uncommon for two or more cases of SjS to occur within a family. Polymorphisms in the major histocompatibility complex (MHC) genes are the best documented genetic risk factors for the development of autoimmune diseases overall (3). In Sjögren's syndrome, the most relevant MHC complex genes are the class II genes, specifically the HLA-DR and DQ alleles (8). However, variations in SjS associated haplotypes amongst different ethnicities, makes it difficult to establish which of the genes confers risk. The severity of the disease also seems to be dependent on the combination of the risk-associated alleles. Sjögren's syndrome patients with DQ1/DQ2 alleles have a much more severe autoimmune disease than patients with any other allelic combination at HLA-DQ (6). Even with specific gene combinations, environmental factors may play a role in the disease onset. Among the possible etiologic factors, viral infections are the most often proposed as a possible trigger of autoimmune disease. Potential viral triggers include Epstein-Barr virus and Hepatitis C. Furthermore, a possible relationship between Sjögren's Syndrome and *Helicobacter pylori* infection has been suspected (2). With these concurrent infections, the risk of mucosa-associated lymphoid tissue lymphoma increases in patients with SjS (2).

Dentists and the ophthalmologists encounter patients afflicted by SjS most often, although a few dermatologists are faced with treating patients presenting cutaneous lesions, in addition to the classic symptoms. A dentist may encounter a SjS patient who complains of dryness in the oral cavity, difficulty swallowing, and a burning sensation in the throat. A patient in the ophthalmologist's office would complain of dryness in the eye, which could lead to infections, keratitis, and sometimes, melting of the cornea or

ocular perforations (5). The cutaneous lesions in patients with SjS are described by dermatologists as palpable and nonpalpable eruptions, pruritic or non-pruritic, as well as symmetric or nonsymmetric in distribution (2). The dermatologist may not recognize these lesions as being associated with SjS and thus, misdiagnose it as Wegener's granuloma. There is still much to be learned about this disease, and once the information is attained it will aid in recognition and treatment of SjS.

Animal Models

The current classification systems provide standards to aid clinicians in diagnosing SjS. However, clinicians are inhibited in their ability to make a diagnosis because the exact onset of the disease is difficult to determine. The onset is usually around forty years of age; however, there are cases of juvenile SjS. Research of SjS within the human population is impeded by the ethical and legal limitations of collecting patients' salivary glands. To study the pathology and etiology of SjS, a variety of mouse models have been developed, such as the New Zealand Black (NZB) and the MRL/n substrains. Today, the mouse used most often is the non-obese diabetic (NOD/LtJ) mouse. The NOD/LtJ (NOD) is characterized as having insulinitis, a leukocytic infiltrate of the pancreatic islets. NOD mice have marked decreases in insulin production by the age of 12 weeks. The NOD/LtJ is considered diabetic when there is moderate glycosuria, and the non-fasting plasma glucose is higher than 250 mg/dl (9). The NOD mouse developed early out of breeding experiments with the Cataract Shionogi (CTS) strain (9). The CTS mice were selected for a high fasting glucose level. From those selected mice a few spontaneously developed overt insulin-dependent diabetes mellitus with insulinitis (IDDM), which is now the NOD/LtJ used today. In the NOD mouse, leukocytic infiltrates and antibodies destroy the pancreatic islets, with exocrine glands infiltrated as well. Of particular interest to SjS

researchers is the observation of lymphocytic foci present in the major salivary gland (submandibular) (10), tear-producing gland (lacrimal) and thymus (11). NOD mice have destruction of the submandibular gland, a marked decreased in salivary flow, and changes in the salivary protein composition. Sera from NOD mice is positive for antinuclear antibodies (SS-A and SS-B), which are detectable by nuclear staining. These symptoms are similar to those seen in humans with secondary Sjögren's Syndrome, thus making the NOD a good mouse model for SjS research.

The pathogenesis of the SjS-like disease seen in the NOD mouse can be divided into two phases. Phase I is a lymphocyte-independent phase where there are abnormalities intrinsic to the submandibular and lacrimal glands of the NOD. Phase II is marked by the autoimmune response via lymphocytic infiltrates in the submandibular (sialoadenitis) and lacrimal (dacryoadenitis) glands, followed by a decrease in tear and saliva production. The lymphocytic infiltrates appear as periductal foci within the glandular architecture of the salivary and lacrimal glands (12). The cause of the autoimmune reaction may reside in the target organ of the autoimmune response, in the immune system, or in both (13). It is theorized that the loss of secretory function is due to lymphocyte-directed destruction. Increased numbers of apoptotic epithelial cells have been detected in the minor salivary glands of patients with SjS (13).

The phase II occurs in the NOD mouse around 10 weeks of age. Current evidence suggests the existence of genetically programmed abnormalities in the exocrine glands of the NOD mouse that may contribute to initiation of the autoimmune reaction (11). Antigen presenting cells, such as dendritic cells, are important mediators of lymphocyte activation, and may respond to organ abnormalities. There is evidence of accumulation of

dendritic cells in the submandibular gland (smg) before the development of lymphocytic infiltrates (13). When these lymphocytic infiltrates form in phase II, dendritic cells interact closely with T-cells, possibly serving to locally activate autoreactive T-cells (11). These organized lymphocytic infiltrates seen in the NOD are also described in the biopsies of SjS patient (14).

As stated before, phase II of SjS is lymphocyte-dependent in humans and the NOD. Research indicates that there is an inappropriate response of dendritic cells to abnormalities of the smg and thus an activation of naïve autoreactive T-cells. These autoreactive T-cells are then capable of stimulating an inflammatory response and autoantibody production. In addition, the dendritic cells of the NOD were found to have a decreased ability to stimulate T suppressor cells (11). T suppressor cells are important regulators of the immune system and have been shown to possess the capacity to alter the stimulation of autoreactive T-cells (15). Infiltrates of exocrine tissues primarily consist of CD4⁺ T-cells with a minority of CD8⁺ T-cell and B-cell populations (12). Studies indicate that activated T-cells, predominantly CD4⁺ T-cells, are necessary for the initiation of autoimmune disease, as indicated by T-cell transfer studies (12). The infiltrates also exhibit aberrant production of the pro-inflammatory cytokines IL- β , IL-2, IL-6, IL-7, IL-10, IL-12, IFN- γ , and TNF- α . Cytokines are important mediators in the immune response, and their altered production can lead to an inappropriate stimulation of lymphocytes.

In addition to the changes in proteins seen in phase I of SjS, there are increases in apoptosis of the submandibular gland acinii (13). Apoptosis, otherwise known as programmed cell death, is an important inhibitory mechanism of cell growth, aiding in

organogenesis, maintaining tissue morphology, and deletion of autoreactive lymphocytes (16). As seen in Fig. 1-1, apoptosis is a complex pathway with many stimulators, such as Caspase-3, and inhibitors, such as AKT. Apoptosis is highly regulated due to its destructive potential. Evidence shows that apoptotic cells can induce inflammation and/or result in the formation of cryptic epitopes (13). Previous studies show increased levels of apoptosis in the *scid* mouse and the NOD, compared to the BalB/c and young NOD (17). The increased levels of apoptosis in the *scid* mouse, indicate that apoptosis may be one of the regulatory abnormalities of the submandibular gland present in phase I (18). The increased cysteine proteases in the *scid* mouse implies that apoptosis is lymphocyte-independent in phase I. However, cysteine proteases have been shown to increase in activity as the NOD aged from 8 weeks to 20 weeks, with the *scid* mouse showing the highest level of activity (17).

The humoral response plays an important role in phase II of SjS. In addition to the SLE antibodies (SS-A and SS-B), anti-M₃ muscarinic acetylcholine receptor autoantibodies have been identified in humans (19) and the NOD mouse (17). SS-A and SS-B are antibodies targeted to antigens that are usually confined to the nucleus (20); however, due to certain events in phase I of SjS these antigens may be presented to the immune system. Muscarinic acetylcholine receptors are important in the secretory function of mammalian exocrine glands. The muscarinic-cholinergic receptor is stimulated by neurotransmitters, resulting in a signal transduction that allows fluid secretion from the salivary gland acinar cells (17). The interaction between an anti-M₃ antibody and the M₃ receptor may result in down-regulation of receptor density, as well as postreceptor second messenger pathway signaling events necessary for proper

activation of fluid movement through epithelial cells (20). In studies where the anti-M₃ antibody and other autoantibodies were introduced into mice lacking the adaptive immune response (*scid* mutation), the anti-M₃ antibody was the only antibody capable of inhibiting secretory function (20). The development of autoantibodies could be a primary immunological response or a secondary effect. In the case of SjS, it is most plausible that the presence of autoantibodies is a secondary effect of the immune system activation (17). Interestingly, many of the autoantibodies are targeted to cell surface proteins important in the secretory response (20), possibly explains why other areas (skin, lungs, GI tract and vaginal tissues), besides the smg and lacrimal glands, are affected in SjS.

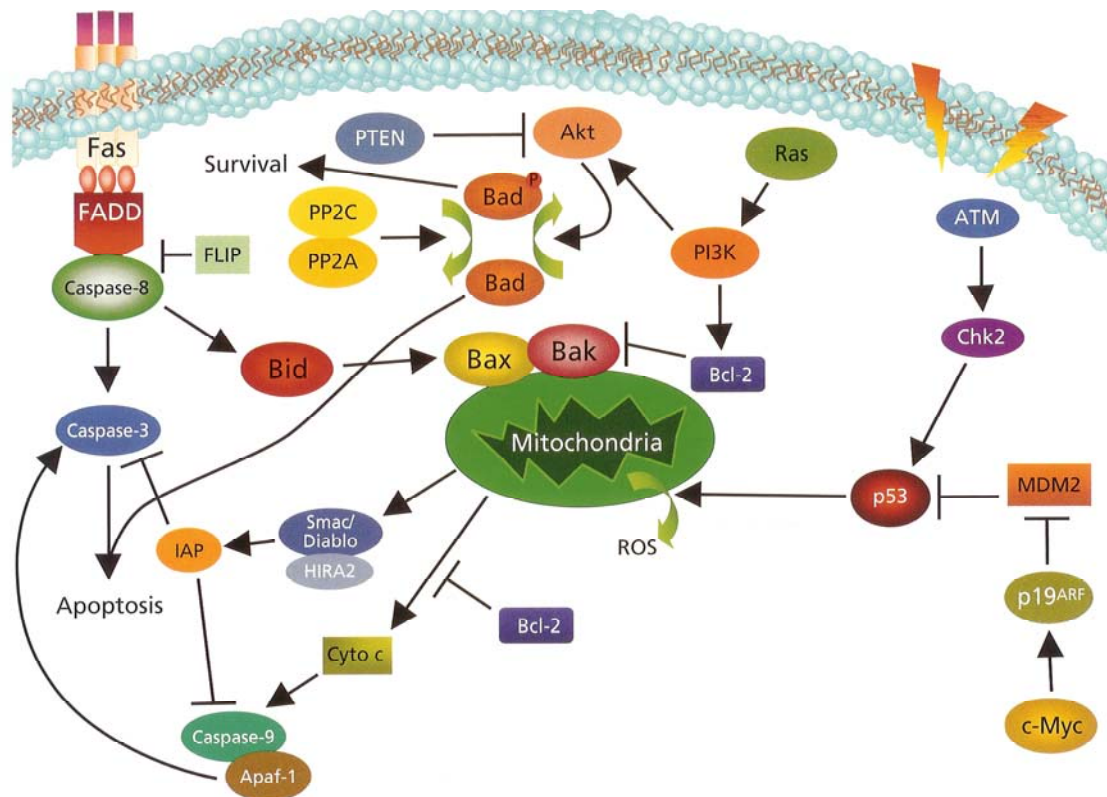


Figure 1-1. Apoptosis pathway. Notice that AKT is an inhibitor early in the pathway and Caspase-3 one of the last activated caspases (16).

The NOD mouse has allowed researchers insight into the phase I of SjS, plus the subsequent development of clinical manifestations. However, a multitude of factors important in the initiation and progression of the disease are not known. Through the development of congenic NOD strains, specific aspects of SjS can be studied. The NOD.CB17-Prkdc*Scid*/J (*scid*) mouse is a congenic mouse that was developed by backcrossing the immunodeficiency locus (*scid*) onto the NOD genetic background. The *scid* locus confers a functional loss of the B and T lymphocytes, otherwise the NOD-*scid* mouse retains the genetic profile of the NOD/LtJ. The NOD-*scid* mouse clarifies the significance of the genetic background in the initiation of SjS, as well as the role of lymphocytes in the clinical manifestations. In addition, the *scid* mouse is capable of accepting allogenic and xenogenic grafts, making it a good mouse model for adoptive cell transfer studies.

There is evidence of intrinsic factors present in the salivary glands of the NOD mouse that are capable of triggering an autoimmune response (14). Analysis of the NOD-*scid* mouse can clarify the role genetics has in the onset and progression of the disease. During phase I, the NOD-*scid* mouse shows a morphological change in the salivary glands, involving a loss of acinar cells within the submandibular glands. The loss of acinar cells increases with age and may be due to either hyperproliferation of the submandibular ductal cells, or apoptotic events (21). However, there are dramatic increases in cysteine protease activity (enzymes important in programmed cell death) in the submandibular glands of older NOD mice and NOD-*scid* mice (12). While the *scid* mouse depicts the same glandular changes as the NOD mouse, the salivary flow rate does not decrease in the *scid*. It is possible; therefore, that there is compensation by the minor

salivary glands (parotid, sublingual, and those in the oral mucosa), resulting in a stable saliva production (21). Nevertheless, data strongly suggest that lymphocytes are necessary for disease progression and the loss of secretory function. Although salivary flow remains stable, there are changes in its composition. The composition of salivary proteins, as shown by epidermal growth factor (EGF) and amylase concentrations in NOD-*scid* saliva, show significant changes with age (21). There is also a novel expression of PRP and an internally cleaved PSP isoform (27 kDa), prominent in 15-week-old NOD-*scid* mouse saliva, but not detected in normal BALB/c mice or younger NOD-*scid* mice (21). These protein changes are similar to those observed in the NOD/LtJ. Interestingly, the time at which this new isoform of PSP appears in the saliva and submandibular glands of NOD-*scid* mice coincides with the appearance of lymphocytic infiltrates in the salivary glands of NOD mice (21). It is possible that the new isoform of PSP, intrinsic to the NOD mouse and its progenitors, may present as a “foreign antigen” to the NOD immune system, thus initiating the autoimmune response. In the NOD mouse, there is stimulation of autoreactive T-cells and autoantibodies. The stimulation of both branches of adaptive immunity may result in the progression of the disease to phase II of SjS.

The NOD-*scid* aids in clarifying the roles of genetics and lymphocytes in the initiation and progression of SjS. It is been made clear, by observing the *scid* mouse, that lymphocytes are important in the loss of saliva secretion. However, the mechanism by which lymphocytes affect the salivary gland function is unclear. There are a few factors of the immune system that may separately, or collectively, inhibit saliva secretion. There is evidence of apoptotic activity in the salivary glands in the NOD mouse (13). The NOD

shows the presence of antibodies specific to exocrine gland receptors, which are capable of reducing salivary flow (20). As stated previously, there are a variety of aberrantly expressed cytokines. The possible pathological effects of these immune responses, provide a range of areas to be researched. In order to study the different immunological aspects, we examined congenic, NOD-derived strains. Two interesting strains used in this study are the NOD.Igh6^{tmlCgn}, commonly known as NOD.Igμ^{null} and for convenience in this thesis, Igμ^{null}, and NOD.129P2(B6)-*Il4*^{tmlCgn}/DvsJ, commonly know as NOD.IL-4^{-/-} and for convenience in this thesis, IL-4^{-/-}.

The NOD.Igμ^{null} mouse is a congenic partner strain of the NOD mouse that is deficient in B-cells. This mouse was developed by disrupting one of the membrane exons of the gene encoding the μ-chain constant region by gene targeting in mouse embryonic stem cells (13). NOD.Igμ^{null} mice exhibit glandular abnormalities of the NOD. Aberrant PSP production is present, but exocrine gland dysfunction (xerostomia, keratoconjunctivitis) does not occur (21). These data imply that B-cells have a significant role in the appearance of xerostomia and keratoconjunctivitis sicca. The B-cell may be an important antigen presenting cell, capable of stimulating autoreactive T-cells. The B-cell also produces autoantibodies present in the NOD mouse and patients with SjS. Transfer of serum from human patients into the Igμ^{null} mice results in a decrease in salivary flow, thus providing evidence that the B-cell is important as an antibody producer, rather than as an antigen presenter (22). This also implies a role for autoantibodies as the effector mechanism for secretory inhibition.

The NOD mouse has a cytokine profile that is specific to the appearance of infiltrates in the salivary glands. The cytokines present consist of interferon (IFN)-γ,

tumor necrosis factor (TNF)- β , IL-1 β , IL-2, IL-6, IL-12 and IL-18, but usually lacking detection of IL-4 (23). Due to its absence, IL-4 has been disregarded as important in progression of the disease. However, the increasing evidence of autoantibodies as an effector mechanism of secretory loss supports a possible role for IL-4 in development of phase II of SjS. The IL-4 cytokine regulates the B-cell maturation and the switch from the IgM to IgG₁ antibody. NOD.IL 4^{-/-} mice exhibit aberrant glandular formations, the novel PSP isoforms, and glandular infiltrations. However, the IL-4^{-/-} mouse does not exhibit the loss of salivary flow. The B-cells, unable to class switch, can not produce autoantibodies specific to exocrine gland receptor, such as the M₃R. This findings support the theory that the humoral response is the mechanism by which exocrine gland secretion is disrupted.

Adoptive Transfer Studies

The use of various gene knockout NOD strains allow different aspects of the disease to be investigated. The NOD-*scid* clarifies the roles of genetics and the immune response. In addition, the roles of B-cells and the IL-4 cytokine are elucidated by observing the NOD.Ig μ ^{null} and NOD.IL-4^{-/-}. All of these strains have the glandular abnormalities and protein production characteristic of phase I of SjS, but development of xerostomia or keratoconjunctivitis does not occur. These observations, as well as serologic analysis of the NOD mouse and patients with SjS, suggest that the humoral response is a pathologic mediator of SjS. By utilizing the adoptive transfer model, the introduction of a combination of lymphocytes into the NOD-*scid* mouse, we hope to identify immune cells important in the role of autoantibody production in the immunopathology of SjS.

The adoptive transfer model, using the NOD-*scid* mouse, was originally developed to study the etiology of diabetes in the NOD/LtJ. Islet-infiltrating lymphocytes, as well as

splenic lymphocytes from NOD mice, can initiate diabetes when transferred into NOD-*scid* mice (24). In those studies, lymphocytes were collected from pre-diabetic and diabetic mice. The pre-diabetic and diabetic lymphocytes were transferred separately, and also as a heterogeneous pool, into NOD-*scid* recipients. The incidence of diabetes in the recipient NOD-*scid* was approximately 70%, similar to the NOD/LtJ control, when splenic lymphocytes from diabetic NOD mice were transferred into NOD neonate recipients (pre-diabetic and pre-SjS) (18). At 12 weeks of age, 50% of the recipient NOD mice showed submandibular gland infiltrations (18). Lymphocytes from the NOD/LtJ also initiate sialoadenitis in the *scid* mouse, but these findings do not identify the role of the humoral response in the cessation of salivary secretion.

The congenic NOD.IL-4^{-/-} mouse does not develop SjS. T-cells from the IL-4^{-/-} mouse are not capable of stimulating isotype switching in B-cells and consequently the IgG₁, anti-M₃R antibody is absent from its sera. In a preliminary study, NOD.IL-4^{-/-} mice were intraperitoneally injected with splenic T lymphocytes from NOD.Igμ^{null} or NOD.IL 4^{-/-} mice (23). This resulted in a decrease of salivary flow in 66% of the Igμ^{null} – T cell recipients, in contrast to the stable salivary flow of the IL 4^{-/-} - T cell recipient (23). The inherent inability of IL 4^{-/-} mice to develop SjS implies that the T-cell's main role in disease progression is as an activator of isotype-switching in B-cells. This theory is further supported by the progression of xerostomia elicited by adoptively transferred splenic T-cells. As shown in a previously mentioned study, NOD.Igμ^{null} T-cells are capable of stimulating autoantibody production. However, the Igμ^{null} mouse does not develop xerostomia. The absence of xerostomia was reversed by transfer of human serum IgG, from Sjögren's Syndrome patients, into the Igμ^{null} mouse (22). Therefore, a logical

conclusion from these data, is that the humoral response appears to be a necessary and sufficient mediator of xerostomia. In order to clarify the causal effect of B-cells and T-cells in Sjögren's Syndrome, the research of this thesis seeks to fulfill the following specific aim:

1. Adoptively transfer different combinations of splenic lymphocytes from the NOD/LtJ mouse and its congenic strains, NOD.Igμ^{null} and NOD.IL 4^{-/-} into the NOD-*scid* mouse in order to establish the adoptive transfer model for phase II of SjS.

To verify the establishment of SjS in these adoptive transfer mice, I have examined:

- The salivary flow and enzyme activity within the saliva of the treated *scid* mice.
- The submandibular gland of the treated *scid* mice to detect the presence of apoptotic events, using flow cytometry, cysteine protease activity, in situ staining, and protein expression via polymerase chain reaction.

CHAPTER 2 MATERIALS AND METHODS

Animals

Animals used in this study were NOD-*scid* (experimental - recipient), NOD/LtJ (experimental - donor), NOD.IL 4^{-/-} (experimental - donor), NOD.Igμ^{null} (experimental - donor), and NOD-*scid* (negative control), and NOD/LtJ (positive control). Female mice were used in all experiments. The donor mice were 16 weeks of age, while the recipient and control mice were 12 weeks old at the time of adoptive transfer. Each treated set includes 4 recipient mice (NOD-*scid*), 2 positive control mice (NOD/LtJ), and 2 negative control mice (NOD-*scid*). Most of the NOD-*scid* mice were purchased from Jackson Laboratory (Bar Harbor, Maine). The other NOD-*scid* mice and the NOD/LtJ, NOD.IL 4^{-/-}, NOD.Igμ^{null} were purchased from the University of Florida, Department of Pathology Mouse Colony (Gainesville, FL) and were housed in the Department of Pathology Mouse Colony under specific, pathogen free conditions.

Adoptive Transfer

The donor mice were euthanized by cervical dislocation and their spleens extracted. The spleens were then pressed through a wire mesh in order to separate the splenic lymphocytes. The lymphocytes were collected and the erythrocytes lysed with 0.84% NaCl. The cells were then washed and incubated for 30 min with the appropriate antibody. Antibodies used were anti - CD19 FITC, anti - CD3 APC and anti - CD25 PE. All antibodies were from BD Pharmingen. After incubation the cells were washed and diluted to a concentration of 8×10^6 cells/ml in 2% FBS in PBS. The lymphocytes were

then sorted by Douglas Smith at the University of Florida, Flow Cytometry Core Laboratory. CD19⁺ - B-cells and CD3⁺CD25⁻ - T-cells were collected. The fractionated splenic lymphocytes were then washed and placed in 100µl 1X Phosphate Buffered Saline. The fractionated splenic lymphocytes were intravenously injected into the recipient *scid* mice in a 1 to 1 ratio (B-cells to T-cells). Each recipient mouse received approximately 3 x 10⁶ cells. The experimental and control mice were divided into two sets of 8 mice (4 experimental *scid* mice, 2 positive control NOD mice, and 2 negative control *scid* mice). One set was observed for 4 weeks, post-transfer (housed until 16 weeks of age), before being euthanized. The other set was observed for 8 weeks, post-transfer (housed until 20 weeks of age) and then euthanized. The submandibular glands, spleens and pancreas of the euthanized mice were collected. The submandibular glands were sectioned into 3 fractions. One section was placed in 2 ml microcentrifuge tubes on ice, for flow cytometry analysis. The next section was placed in cassettes, stored in 4% Formalin overnight, and then placed in 70% EtOH to be formed into paraffin-embedded blocks. The last section was placed in 2 ml microcentrifuge tubes and frozen with dry ice. The frozen tubes were then stored in at -80°C for future analysis.

Saliva Collection

Saliva was collected from the experimental (NOD-*scid*), positive control (NOD/LtJ), and negative control (NOD.IL 4^{-/-}). The salivary glands were stimulated with secretagogues to induce salivation. The secretagogue solution is composed of Isoproterenol (1mg/ml) and Pilocarpine (2mg/ml) (Sigma) in 1X Phosphate Buffered Saline. Each mouse received 100 µl of the secretagogue via an intraperitoneally injection. The saliva was stimulated for 1 minute and then collected by pipetting for 10 minutes. The collected saliva was placed in 1.5 ml microcentrifuge tubes. The volume of saliva

was quantified using pipettors and recorded. The saliva was then stored in a -80°C freezer for future protein analysis.

Protein Concentration

The protein concentration of the collected saliva and submandibular gland lysate was determined, using the Bradford assay. 1 mg of Bovine Serum Albumin (Sigma) was diluted in 1 ml deionized H₂O. The Bradford protein assay dye was then diluted 1:5 in deionized H₂O. The standards and samples were made and later read in 2 ml cuvettes. The 1 mg/ml BSA was diluted with H₂O, to a total volume of 25 µl, to make the following standards: 0 mg/ml, 5 mg/ml, 10 mg/ml, 15 mg/ml, and 20 mg/ml. For each sample, 5 µl of sample and 20 µl of H₂O was added to each cuvette. 1 ml of the diluted Bradford dye was added to each cuvette, and mixed with a pipette. The standards and samples were allowed to incubate for 5 minutes at room temperature. The protein concentration was detected using the protein concentration program available in the spectrophotometer (Bradford). The standards were used to make a standard curve and then the protein concentrations of each sample extrapolated from the standard curve.

Amylase Activity Analysis

Detection of amylase present in collected saliva and submandibular gland lysate was accomplished by using the Infinity Amylase Reagent (ThermoTrace). Amylase activity is detected via utilization of Ethylidene-pNP-G7 (EPS) as the substrate. The cleaved EPS reacts with α -glucosidase, resulting in release of a chromophore. The color change is then detected at 405nm in a spectrophotometer (BioRad). Amylase activity is defined as the rate of formation of EPS fragments per liter of sample (U/L). The saliva samples were diluted 1:200 in deionized H₂O. The submandibular gland lysate were analyzed undiluted. However a few gland lysate samples had an amylase activity that

was unmeasurable when not diluted. These samples were diluted 1:100 in H₂O. 1 ml of Infinity Amylase reagent was added to a cuvette and incubated in a waterbath set at 37°C for 1 min. 25 µl of diluted sample was then added to the heated reagent and incubated for 1 min. After the 1 min incubation was completed, the timer for the next incubation minute is started. The reagent/sample was mixed with a pipette and read in the spectrophotometer to obtain the initial reading. Afterwards the reagent/sample was placed in the waterbath until the incubation time is complete. The timer was started for the final incubation time of 1 min, immediately after the second incubation time was completed. The reagent/sample was read in the spectrophotometer to obtain the second reading. The reagent/sample was placed in the waterbath. At the end of the final incubation time, the reagent/sample was read. The spectrophotometer was blanked with H₂O in the Infinity Reagent. The positive and negative controls were obtained from the provider of the amylase reagent (Thermotrace) and treated the same as the samples. From this assay, three O.D. readings are obtained. The change in amylase activity is obtained by subtracting the initial O.D. reading from the final O.D. reading and dividing by the amount of incubation time between the initial and the final reading (2 min). The obtained value is then multiplied by the conversion factor (5140). The conversion factor is calculated based on manufacturer instructions. The amylase activity of each sample (U/L) is then divided by the known protein concentration (µg/L), and then multiplied by 1×10^4 to standardize. The resulting amylase activity is measured as the rate of formation of EPS per gram of protein (U/gram of protein). The assay was performed three times in order to obtain statistical analysis.

Apoptosis Detection

Apoptosis Detection via Flow Cytometry

The day the collected submandibular glands are retrieved from the experimental and control mice, the glands are digested. The submandibular glands are minced and placed in a vial with 5 ml of Collagenase Solution I (2 mg/ml of collagenase IV (Sigma) in 1X Hanks Balanced Salt Solution (HBSS) and 200 μ l of Dnase). The vials were then placed in a shaking waterbath, set at 37°C, for 15 minutes. The partially-digested glands were passed through a series of syringes with needles increasing in gauge, from 18 to 23. The digested glands were then placed in a vial with Collagenase Solution II (1 mg/ml of collagenase in 1X HBSS with 200 μ l of Dnase). The glands were incubated in a shaking waterbath for 5 min. The digested gland mixture was passed through a series of syringes again. At this point the glands should be fully digested. The submandibular cells were placed in 50 ml conical tubes containing 2% FBS in 1X HBSS and placed on ice. The submandibular cells were collected after centrifugation and counted. The submandibular cells were diluted with 1X PBS to a concentration of 1×10^6 cells/ml. In sterile 12 ml plastic tubes, 5 mls of 55% Percol was added and 2 mls of the diluted, digested glands were carefully layered on top with siliconized pipettes. The tubes were centrifuged for 30 min at a speed of 2,000 rpms. After the gradient separation the acinar cells and infiltrates were collected with siliconized pipettes and placed in 12 ml plastic tubes. The cells were washed and counted. The acinar and infiltrates were then placed in a sterile culture plate with a solution containing 2% FBS in RPMI (Sigma) and 1X antibiotics. The cells were cultured overnight to allow the cells to recuperate. The following day, the acinar and infiltrate cells were fixed in 1 % paraformaldehyde in 1X PBS for 15 min on ice. The cells were washed and placed in 5 ml flow cytometry tubes with 70% ETOH. The tubes

were placed in a -20°C freezer to be stored for 24 hrs. The fixed cells were washed in preparation of staining by reagents provided in the APO-Direct kit (BD Pharmingen). This assay utilizes a TUNEL labeling system, where terminal deoxynucleotidyl transferase enzyme (TdT) enables the template independent addition of FITC labeled deoxyuridine triphosphate nucleotides (FITC-dUTP) to DNA strand breaks present in apoptotic cells. Propidium Iodide (PI)/RNase solution was used to stain total DNA. Apoptotic cells were provided by the kit as a positive control, as well as non-apoptotic cells as a negative control. After staining, following the procedure outlined by manufacturer specifications, the cells were incubated in Propidium Iodide and analyzed by flow cytometry. Manufacturer suggestions were used as a guide to determine appropriate parameters for apoptosis detection. Cells were identified as apoptotic if they expressed FITC-dUTP. The parameters for positive apoptosis was based on the level of positivity determined by the positive and negative control. A window was selected that included positive control cells that express dUTP, but excluded negative control cells. In order to analyze and standardized the results, the following formula was used: $(\% \text{pos. cells sample } x - \% \text{ pos. cells in the neg. control}) / \% \text{ pos. cells in pos. control}$. Using the aforementioned formula, substituting the %pos. cell sample x with the %pos. cells positive control (provided in the kit), will standardize the positive control as 100% positive. The same formula is applied to the negative control (provided in the kit) so that the level of positivity is 0%. The equation is applied to each sample and the positivity determined. For comparison, the relative positivity in each treated set is assigned a representative value on a scale from 0 to 10 (0 is equal to 0% positive and 10 is equal to 100% positive).

Akt Expression via Polymerase Chain Reaction

The stored experimental and control submandibular glands were removed from the freezer and 25 mg of tissue removed. The sectioned piece of submandibular gland was then treated according to manufacturer specifications to extract total RNA (Qiagen). The extracted total RNA was then quantified in the spectrophotometer. A quartz cuvette was used and the spectrophotometer was blanked with deionized water. The total RNA was diluted 1: 50 in deionized water and read in the spectrophotometer. Only total RNA with at least a concentration of 800 $\mu\text{g/ml}$ were used to produce cdna. To a .02 ml nuclease-free centrifuge tube the reagents were added in the following order; 1 μl of pd(T)₁₂₋₁₈, 1 μl of 10 mM dNTP, 1 μg of total RNA, and enough water so that the total volume in the tubes equal 10 μl . After mixing, the tubes were heated in a waterbath for 5 min at 65°C and quick chilled on ice. The tubes were then centrifuged and the reagents added in the following order; 4 μl of 5X First-Strand buffer, 2 μl 0.1M DTT, 1 μl RNasin, and 2 μl acetylated BSA. After gentle mixing, the tubes were incubated in a waterbath, and set at 42° C for 2 minutes. To each tube 1 μl of SuperScript II was added and mixed gently. The tubes were incubated at 42° C for 50 minutes and then 70° C for 15 minutes in the thermocycler. The cdna concentration was quantified by the spectrophotometer. A quartz cuvette was used and the spectrophotometer blanked with deionized water. The cdna was diluted 1 : 50 in deionized water and read in the spectrophotometer. A master mix was made by adding the following reagents to a 2 ml nuclease-free centrifuge tube; 5.1 μl 10X Buffer, 1.1 μl 10 mM dNTPs, and 1.6 μl of MgCl₂ (formula is for one pcr reaction). 7.5 μl of the master mix was added to a .02ml nuclease-free centrifuge tube. To each .02 ml pcr tube the following reagents were added; 1.5 μl of the forward primer, 1,5 μl of the reverse primer, 2 μg of cdna, and enough water so that the volume of the

microcentrifuge tube equals 49.75 μ l. The primer sets used were 18S (housekeeping gene) and AKT. Both primer sets were individually developed by Invitrogen. The tubes were mixed, centrifuged and incubated in a thermocycler, following the standard program for polymerase chain reaction. The annealing temperature was set at 57.2°C. After the denaturation step, but before the 1st annealing temperature is reached, .25 μ l of Taq DNA Polymerase (Invitrogen) is added to each tube. The PCR reaction is then continued in the thermocycler.

Agarose Gel Electrophoresis

A 2% TBE, agarose gel was made and 5 μ l of ethidium bromide added to the gel while it was still warm. After the gel set, the previously made PCR products were defrosted. 12 μ l of 18s amplicons and 3 μ l of 6X Blue/Orange Dye (Promega) were added per well. In the lane above, 24 μ l of akt amplicons and 4 μ l of 6X Blue/Orange Dye (Promega) were loaded into each well. 1 μ l of the PGEM[®] DNA marker (Promega), 4 μ l of dye and 23 μ l of 1X TBE was loaded into a well. The TBE gel was then run at 70 volts for 1.5 hr. Afterwards, the gel was visualized with a gel document system, and quantitative analysis done using the AlphaEase FC program (Alpha Innotech). The level of akt expression per sample is based on the samples corresponding level of 18s expression. 18s is ubiquitous in all cells and should; therefore, all samples should have the same amount of expression. However slight variations in the level of expression occurs. Within each lane of a gel are many samples. To standardized the values for 18s expression, a ratio is formed by dividing highest 18s value within that lane by the 18s value for each sample within the same lane. The inverse of the calculated 18s ratio (highest 18s/18s of sample x) is then multiplied by the corresponding akt expression

value (inverse of 18s ratio of sample x, multiplied by akt of sample x). From these calculations a relative, qualitative expression value is obtained.

Caspase-3 Activity Detection

Stored submandibular glands were defrosted on ice and homogenized with 600 μ l of Tris-HCL, ph 8.0 in 5 ml plastic tubes. The gland lysate was transferred to 2.0 ml microcentrifuge tubes. The gland lysate was then assayed following manufacturer specifications (Calbiochem). The activity assay was read in a microplate reader for 20 minutes and the values calculated in Excel. The data points were plotted on a graph, activity (x axis) vs. time (y axis), and a trendline generated. The slope of the trendline was then multiplied by the conversion factor (conversion factor tabulated as suggested by kit).

In Situ Apoptosis Detection Kit.

The previously paraffinized submandibular glands were sectioned and placed on slides by Histology Technical Services. The slides were then deparaffinized by incubation in a series of solutions in the following order: two incubations in Xylene for 5 min, two incubations in 100% EtOH for 2 min and two incubations in 95% EtOH for 2 min, two incubations in 70% EtOH for 2 min, two incubations in H₂O for 2 min. The slides were then stained, following manufacturer specifications (Trevigen), in a humidity chamber. After the slides were dehydrated, the tissues were covered with a non-aqueous mount and a coverslip added. The slides were allowed to dry overnight and then viewed under brightfield microscopy.

Detection of Infiltration

Immunohistochemistry

The paraffinized submandibular slides were obtained as stated previously. They were deparaffinized (as stated previously) and placed in a heated coplin jar, containing 1X antigen unmasking solution (Trevigen). The coplin jar was then incubated in a waterbath for 30 min at 95°C. The slides were then washed with H₂O and placed in a humidity chamber. The slides were equilibrated with the buffer, 1X TBST (Dako) for 5 min. 200 µl of diluted (1:67) goat serum (Sigma) was pipetted onto each slide and incubated for 20 min at room temperature. The goat serum was carefully wiped off the slide, so that the tissue remained undisturbed. The slides were then incubated for 1 hr with 200 µl diluted (1:25) B2-20 antibody (BD Pharmingen), at room temperature. The slides were then washed with 1X TBST for 5 min and incubated with 200 µl of diluted (1:200) anti-rat antibody (Sigma), for 30 min. Before the diluted anti-rat antibody is added to the slides approximately 5 µl of mouse serum is added to the 2° antibody solution. The slides are washed with 1X TBST and treated with an ABC - alkaline phosphates kit from Vector Labs. The slides were treated with reagents as specified by the manufacturer (Vector Labs). The substrate used in the alkaline phosphates system was Vector Red (Vector Labs). The substrate was mixed following manufacturer specifications and incubated on the slides for 20 min. The slides were then washed in deionized H₂O for 1 min and then washed with 1X TBST for 5 min. The slides were incubated with 200 µl of diluted (1:67) rabbit serum (Sigma) for 20 min. The slides were then incubated with 200 µl, diluted (1:125) CD3 antibody (Santa Cruz), overnight at 4° C. The slides were then washed with 1X TBST for 5 min, and incubated with 200 µl of diluted (1:200) α-goat antibody (Sigma) for 30 min. The slides were then treated with the

reagents provided in the ABC – immunoperoxidase system (Vector Labs). The slides were treated as specified by the manufacturer. DAB (Vector Labs) was used as the substrate, and was mixed as specified by the manufacturer. The slides were incubated with the DAB for 5 min. The slides are then washed in H₂O for 1 min. The slides are immersed in a working solution of the Light Green Counterstain (Sigma) for 1 min. The slides are then immersed twice in H₂O for 1 min. The slides are then dehydrated by being immersed in a series of solutions for 2 min; 70% EtOH, 95% EtOH, 2 times in 100% EtOH and followed by immersion in Xylene for 5 min, 2 times. Afterwards the slides are coverslipped and visualized by brightfield microscopy. The presence of lymphocytes is determined as cells that positively stained with Vector Red (T-cells) and DAB (B-cells)

CHAPTER 3 RESULTS

Adoptive Transfer

Purified splenic lymphocytes from certain donor mice were labeled with the appropriate fluorescent conjugated antibody (except for the unfractionated donor NOD/LtJ splenocytes) and sorted by flow cytometry. The collected splenocytes were selected based on the level of binding to the conjugated antibody. The splenocytes were collected in two separated fractions. Selected B-cells depicted a high level of CD19⁺ FITC expression. Selected T-cells depicted a high level of CD3⁺ APC while showing no CD25⁺ PE expression. CD25⁺ T-cells have shown to have a protective quality in adoptive transferred of diabetes studies (25). To circumvent inhibition of disease transfer, the CD25⁺ phenotype was set as a negative selection parameter. The purity of the collected splenocytes was analyzed by flow cytometry. Each fraction had a purity of approximately 93%. The collected splenocytes were then washed and intravenously injected into the recipient NOD-*scid*. Each *scid* received an average of 3×10^6 B and/or T-cells.

The donor splenocytes were selected based on their expected contribution to the development of SJS. The T-cells and B-cells from the NOD/LtJ were selected because they should transfer the disease to the *scid*. The T-cells of the I μ ^{null} was selected due to its shown ability to stimulate an autoreactive B-cell, thus transferring the disease. The B-cells from the NOD.IL 4^{-/-} should interact with a normal T-cell, resulting in transfer of the disease. Those *scid* mice that received T-cells or B-cells, but not both, are expected to exhibit no disease transfer.

Table 3-1. Adoptive transfer, combinations of donor splenocytes transferred to the *scid*.

Recipient	Donor T-cells	Donor B-cells	Pos. Control	Neg. Control
NOD- <i>scid</i>	Total spleen	Total spleen	NOD/LtJ	NOD- <i>scid</i>
NOD- <i>scid</i>	Total spleen	Total spleen	NOD/LtJ	NOD- <i>scid</i>
NOD- <i>scid</i>	NOD/LtJ	NOD/LtJ	NOD/LtJ	NOD- <i>scid</i>
NOD- <i>scid</i>	NOD/LtJ	NOD/LtJ	NOD/LtJ	NOD- <i>scid</i>
NOD- <i>scid</i>	NOD/LtJ	NOD.IL4 ^{-/-}	NOD/LtJ	NOD- <i>scid</i>
NOD- <i>scid</i>	NOD/LtJ	NOD.IL4 ^{-/-}	NOD/LtJ	NOD- <i>scid</i>
NOD- <i>scid</i>		NOD.IL4 ^{-/-}	NOD/LtJ	NOD- <i>scid</i>
NOD- <i>scid</i>		NOD.IL4 ^{-/-}	NOD/LtJ	NOD- <i>scid</i>
NOD- <i>scid</i>	NOD.Igμ ^{null}	NOD.IL4 ^{-/-}	NOD/LtJ	NOD- <i>scid</i>
NOD- <i>scid</i>	NOD.Igμ ^{null}	NOD.IL4 ^{-/-}	NOD/LtJ	NOD- <i>scid</i>
NOD- <i>scid</i>	NOD.Igμ ^{null}		NOD/LtJ	NOD- <i>scid</i>
NOD- <i>scid</i>	NOD.Igμ ^{null}		NOD/LtJ	NOD- <i>scid</i>
NOD- <i>scid</i>	NOD.Igμ ^{null}	NOD/LtJ	NOD/LtJ	NOD- <i>scid</i>
NOD- <i>scid</i>	NOD.Igμ ^{null}	NOD/LtJ	NOD/LtJ	NOD- <i>scid</i>

Saliva Collection

A significant manifestation of SjS in the NOD/LtJ mouse is the presence of xerostomia. Xerostomia in the recipient *scid* was detected by quantifying the volume of saliva produced in 10 minutes. Salivation was stimulated by secretagogues and the saliva collected from 4 treated *scid* mice, 2 positive control NOD mice and 2 negative control *scids*. The collected saliva from the 4 treated mice, per group, was pooled. The collected saliva from the pos. control was pooled, and the neg. control saliva was pooled as well. Saliva was collected once a week for 7 wks, but many mice were euthanized early. Diabetes, which is present in the NOD, was transferred along with the SjS. The mice that became diabetic were treated with insulin, but many expired early. To circumvent the loss of all experimental mice; many diabetic *scids* were euthanized early.

The collected saliva from 4 week post transfer was compared to the volume of saliva from the last week of collection. As seen in Table 3-2, the *scid* (Unfractionated NOD) did not show a change in salivary flow. The *scid* (B and T – NOD) expressed a decrease of 46%, which is comparable to previous data on the NOD. The

scid (B – IL4^{-/-} and T – NOD) showed a 68% decrease in flow. The *scid* (B – IL4^{-/-}) showed a small decrease of 13%. The *scid* (T – I μ ^{null} and B – IL4^{-/-}) and *scid* (T – I μ ^{null}) showed a increase of about 35%. The *scid* (T – I μ ^{null} and B – NOD) had a small increase of 9%. The *scid* mice that were recipients of either T or B – cells, but not both, had a stable flow, similar to the NOD-*scid*. Surprisingly, none of the NOD mice depicted xerostomia. The NOD, in previous studies, has proven to be a good positive control for SjS, so this was certainly an unexpected occurrence.

Amylase Activity Analysis

Amylase Activity Detected in Saliva.

An important aspect of SjS is the aberrant production of salivary components such as amylase. The collected saliva was analyzed to determine the amylase activity of the saliva. As shown in Table 3-2, the amylase activity of mice 4 weeks post-transfer (16 week old mice) was compared to the activity of mice 8 weeks post-transfer (20 week old mice). The calculated readings showed that the *scid* (Unfractionated NOD) had an increase of 62%, the *scid* (T and B – NOD) amylase activity decreased by 8% and the *scid* (T – NOD and B – IL4^{-/-}) had an increase of 46%. The *scid* (B – IL4^{-/-}) had a decrease in activity of 57%. The *scid* recipients of T-cells from the I μ ^{null} all showed a decrease in amylase activity that ranged from 5% in the *scid*(T - I μ ^{null} and B – IL4^{-/-}) to 33% in the *scid*(T - I μ ^{null} and B – NOD). The NOD control shows a 21% decrease and a 43% decrease in the *scid*.

Detection of Salivary Gland Amylase Activity

An important aspect of the initiator phase of SjS is the change in composition of the submandibular glands. In order to determine if there are changes, the amount of amylase present was analyzed. The submandibular glands were homogenized and the gland lysate

incubated with Infinity Amylase Reagent (Thermotrace) for the appropriate time. The activity was detected in spectrophotometer. As seen in Table 3-3, the *scid* (Unfractionated NOD) and *scid* (T – NOD and B – IL4^{-/-}) exhibited an increase in activity of 300% and 970%, respectively. The *scid* (T and B – NOD) had a decrease of 80%. The *scid* (B – IL4^{-/-}) showed an increase of 500%. The *scid* (T – I μ ^{null} and B – IL4^{-/-}) and the *scid* (T – I μ ^{null} and B – NOD) had a decrease in amylase activity of 90% and 34%, respectively. The *scid* (T – I μ ^{null}) showed a less than 6% increase. The NOD and *scid* showed a decrease in amylase activity of 33% and 25%.

Protein Concentration

A significant aspect of SjS is the aberrant protein production, specifically the production of two novel forms of parotid secretory protein (PSP). The deviant PSP production allows the protein concentration to remain stable, even as other major proteins decrease. Using the Bradford protein assay the protein concentration of saliva and submandibular gland lysate was determined. The protein concentration of the saliva did not show a change in concentration in any of the adoptively transferred *scid* mice or the controls. The adoptively transferred *scid* mice and the controls had an average protein concentration of 3.6 mg/ml, 4 weeks post-transfer. The average protein concentration at 8 weeks post-transfer was 3.8 mg/ml. The submandibular gland lysate depicted a decrease in protein concentration for the *scid* mice that received a combination of T and B-cells. This decrease ranged from 78% in the *scid* (T – NOD and B – IL4^{-/-}) to 22% in the *scid* (T – I μ ^{null} and B – IL4^{-/-}). The *scid* (T – I μ ^{null}) depicted a decrease of 55%. The *scid* (B – IL4^{-/-}), *scid* (Unfractionated NOD) and the controls did not show a change in protein concentration.

Table 3-2. The saliva from each adoptively transferred *scid* was collected and quantified. The saliva was then assayed to determine the amount of amylase present and the concentration of proteins.

Age of treated mouse	Total salivary volume (μl/10 min)	Amylase activity (U/gram of protein)	Total protein (mg/ml)
4 wks – NOD (n = 10)	185	5881 ± 671 ^d	3.72 ± .77
>8 wks – NOD (n = 7)	236	4643 ± 541	3.48 ± .3
4 wks – <i>scid</i> (n = 12)	180	7082 ± 547	3.01 ± .8
>8 wks – <i>scid</i> (n = 12)	216	4051 ± 879	3.21 ± .1
4 wks – <i>scid</i> (Unfractionated NOD) (n = 4)	168	2786 ± 173	3.92 ± .02
>8 wks – <i>scid</i> (Unfractionated NOD) (n = 4)	170	4509 ± 410	4.85 ± .03
4 wks – <i>scid</i> (T and B - NOD) (n = 4)	168	4881 ± 446	3.72 ± .02
>8 wks – <i>scid</i> (T and B - NOD) (n = 2)	90 ^{a,*}	4486 ± 107	4.60 ± .02
4 wks – <i>scid</i> (T – NOD and B – IL-4 ^{-/-}) (n = 4)	125	6055 ± 106	3.63 ± .003
>8 wks – <i>scid</i> (T – NOD and B – IL-4 ^{-/-}) (n = 2)	40 ^b	8846 ± 288 ^{c,**}	2.55 ± .02
4 wks – <i>scid</i> (B – IL-4 ^{-/-}) (n = 4)	200	4282 ± 126	5.02 ± .04
>8 wks – <i>scid</i> (B – IL-4 ^{-/-}) (n = 4)	175	1824 ± 450	5.25 ± .03
4 wks – <i>scid</i> (T- Igm ^{null} and B – IL-4 ^{-/-}) (n = 4)	63 ^{c,*}	7202 ± 443 ^{c,*}	2.93 ± .01
>8 wks – <i>scid</i> (T- Igm ^{null} and B – IL-4 ^{-/-}) (n = 2)	100 ^c	6788 ± 136	3.42 ± .01
4 wks – <i>scid</i> (T- Igm ^{null}) (n = 4)	113	4154 ± 667	3.51 ± .03
>8 wks – <i>scid</i> (T- Igm ^{null}) (n = 4)	150	3160 ± 519	3.06 ± .02
4 wks – <i>scid</i> (T- Igm ^{null} and B – NOD) (n = 4)	110	7091 ± 442	3.02 ± .02
>8 wks – <i>scid</i> (T- Igm ^{null} and B – NOD) (n = 3)	120	4735 ± 397	3.44 ± .01

^a Due to the transfer of diabetes, this set euthanized at week 5.

^b Due to the transfer of diabetes, this set euthanized at week 6.

^c Due to the transfer of diabetes, this set euthanized at week 5.

^d Values are given as the mean ± standard error.

^e Statistical comparison of adoptively transferred NOD-*scid* mouse groups to the age-matched NOD-*scid* parental control by the one way ANOVA test: (*P < 0.05, **P < .001).

Table 3-3. The submandibular glands for the adoptively transferred *scid* mice and the controls were collected and homogenized. The level of caspase activity was determined using the Caspase-3 activity kit. The gland lysate was assayed to determine the amylase present and protein concentration.

Age of treated mouse	Total protein (mg/ml)	Amylase activity (U/gram of protein)	Caspase 3 Activity (pmol/min/gram of protein)
4 wks – NOD (n = 10)	3.4 ± .08	101.2 ± 94	39.8 ± 10 ^a
>8 wks – NOD (n = 7)	4.3 ± .41	67.9 ± .4	31 ± 5.8
4 wks – <i>scid</i> (n = 12)	3.4 ± .02	159.4 ± 30.8	28.4 ± 3.8
>8 wks – <i>scid</i> (n = 12)	4.4 ± .02	119.1 ± 10.2	30.1 ± 6.7
4 wks – <i>scid</i> (Unfractionated NOD) (n = 4)	4.0 ± .04	194.7 ± 94	59.6 ± 3.3 ^{b**}
>8 wks – <i>scid</i> (Unfractionated NOD) (n = 4)	4.2 ± .01	863 ± 433 ^{b**}	26.5 ± 0.3
4 wks – <i>scid</i> (T and B - NOD) (n = 4)	5.2 ± .02 ^{b*}	415 ± 53	29.1 ± .6
>8 wks – <i>scid</i> (T and B - NOD) (n = 2)	1.6 ± .02 ^{b**}	77 ± 4	40.5 ± 0.1
4 wks – <i>scid</i> (T – NOD and B – IL-4 ^{-/-}) (n = 4)	5.4 ± .01 ^{b*}	34 ± 13	34.6 ± .2
>8 wks – <i>scid</i> (T – NOD and B – IL-4 ^{-/-}) (n = 2)	1.2 ± .01 ^{b**}	365 ± 84	265.8 ± 23.8 ^{b**}
4 wks – <i>scid</i> (B – IL-4 ^{-/-}) (n = 4)	2.9 ± .03	137 ± 29	38.6 ± .2
>8 wks – <i>scid</i> (B – IL-4 ^{-/-}) (n = 4)	4.6 ± .02	955 ± 257	44.1 ± .9
4 wks – <i>scid</i> (T- Igm ^{null} and B – IL-4 ^{-/-}) (n = 4)	4.3 ± .01 ^{b**}	409 ± 148	36.5 ± 1.3
>8 wks – <i>scid</i> (T- Igm ^{null} and B – IL-4 ^{-/-}) (n = 2)	1.6 ± .01	43 ± 14	46.8 ± 4.6
4 wks – <i>scid</i> (T- Igm ^{null}) (n = 4)	3.4 ± .02	161 ± 30	28.6 ± 1.1
>8 wks – <i>scid</i> (T- Igm ^{null}) (n = 4)	1.5 ± .01 ^{b**}	170 ± 114	62.8 ± 11.4 ^{b**}
4 wks – <i>scid</i> (T- Igm ^{null} and B – NOD) (n = 4)	5.1 ± .02 ^{b*}	862 ± 153 ^{b*}	31.0 ± 4.7
>8 wks – <i>scid</i> (T- Igm ^{null} and B – NOD) (n = 3)	4.0 ± .01	573 ± 129 ^{b*}	48.3 ± .8

^aValues are given as the mean ± standard error.

^bStatistical comparison of adoptively transferred NOD-*scid* mouse groups to the age-matched NOD-*scid* parental control by the one way ANOVA test: (*P < 0.05, **P < .001).

Apoptosis Detection

Apoptosis Detection via Flow Cytometry

The presence of apoptosis is a significant aspect of xerostomia and is a noted event in disease progression. Apoptosis in the submandibular acinii cells was detected following the protocol provided in the Apo-Direct kit (BD Pharmingen). Apoptotic and non-apoptotic cells were provided as a positive and negative control. The level of positivity for apoptosis was based on the controls. As seen in Table 3-4, apoptosis was not detected in the *scid* (B – IL4^{-/-}) at 4 weeks and 8 weeks post-transfer. Apoptosis was also detected in the *scid* (T – Igm^{null}) at 8 weeks. The NOD mice exhibited a low level of apoptosis at 4 weeks post-transfer with no apoptosis present at 8 weeks. There was no

apoptotic events detected in the *scid* negative control or the experimental *scid* mice at 4 weeks or 8 weeks.

Table 3-4. Apoptosis detection using Apo-Direct kit (BD Pharmingen). The positivity of each sample is based on the positive and negative controls provided in the kit. The samples were standardized by the following formula: (% Pos of sample X – % Pos. of Neg. control)/ (% Pos. of Pos. Control). Numerical values are assigned so that 0/10 is equal to 0% positive for apoptosis and 10/10 is equal to 100% positive.

Recipient NOD- <i>scid</i> (age)	Donor cells	Apoptosis Activity (AU)
NOD/LtJ 4 weeks	Positive Control	1/10
8 weeks		0/10
NOD- <i>scid</i> 4 weeks	Negative Control	0/10
8 weeks		0/10
NOD- <i>scid</i> 4 weeks	Unfractionated NOD	0/10
8 weeks	Unfractionated NOD	0/10
NOD- <i>scid</i> 4 weeks	T- NOD and B- <i>Il4</i> ^{-/-}	0/10
8 weeks	T- NOD and B- <i>Il4</i> ^{-/-}	0/10
NOD- <i>scid</i> 4 weeks	T and B - NOD	0/10
8 weeks	T and B - NOD	0/10
NOD- <i>scid</i> 4 weeks	B - <i>Il4</i> ^{-/-}	7/10
8 weeks	B - <i>Il4</i> ^{-/-}	10/10
NOD- <i>scid</i> 4 weeks	T - <i>Igμ</i> ^{null}	0/10
8 weeks	T - <i>Igμ</i> ^{null}	10/10
NOD- <i>scid</i> 4 weeks	T- <i>Igμ</i> ^{null} and B - <i>Il4</i> ^{-/-}	0/10
8 weeks	T- <i>Igμ</i> ^{null} and B- <i>Il4</i> ^{-/-}	0/10
NOD- <i>scid</i> 4 weeks	T - <i>Igμ</i> ^{null} and B - NOD	0/10
8 weeks	T - <i>Igμ</i> ^{null} and B - NOD	0/10

Caspase-3 Activity Detection

Apoptosis, otherwise known as programmed cell death, is an important inhibitory mechanism of cell growth. Apoptosis aids in organogenesis, maintenance of tissue morphology, and deletion of autoreactive lymphocytes. As seen in Fig. 3-1, there are a series of events that occur in the apoptotic pathway. One of the last events is the activation of caspases. Caspase-3 is a member of the interleukin - 1 β converting enzyme (ICE) family of cysteine proteases. It is activated by a series of upstream proteases and is one of the last signaling events before apoptosis occurs. The submandibular gland lysate samples were analyzed in an enzymatic assay. For each treated set caspase activity was compared at 4 weeks post-transfer to 8 weeks post-transfer. As seen in Table 3-3, the *scid* (Unfractionated NOD) depicted a 55% decrease in caspase activity. The *scid* (T and B - NOD) showed an increase in activity of 40%. The *scid* (T-NOD and B-IL 4^{-/-}) depicted an increase of over 200%. The *scid* (B-IL 4^{-/-}) had an increase of 14% in caspase activity. The *scid* (T-Ig μ^{null}) and the *scid* (T-Ig μ^{null} and B-NOD) both depicted an increase in activity of about 50%. The *scid* (T-Ig μ^{null} and B-IL 4^{-/-}) depicted a slight decrease of 18%. The NOD had a decrease in activity of 22% and the *scid* had a less than 6% increase in caspase activity.

Akt Expression via Polymerase Chain Reaction

As a critical mechanism of homeostasis maintenance, apoptosis also has a large destructive potential, if not closely controlled. As seen in Fig 3-1, there are many proteins capable of inhibiting apoptosis. Akt, also known as protein kinase B, is the protein of interest for this thesis. Akt inhibits apoptosis by phosphorylating, and thus inactivating procaspases, Bad, and other transcription factors. The level of akt expression is determined by amplifying cdna, from each sample, by polymerase chain reaction. The

polymerase chain reaction products are visualized by gel electrophoresis. The level of expression is tabulated for 18s pcr products (housekeeping gene) and the akt pcr products, using the AlphaEase FC program. The relative expression of akt of each treated sample is then compared to the NOD (pos. control) and the *scid* (neg. control), to form ratios. The sample/*scid* ratio is then compared to the sample/NOD ratio to determine the relative increase in expression from 4 weeks to 8 weeks post-transfer. As shown in Table 3-5, the *scid* (Unfractionated NOD) depicted an increase in akt expression when compared to the NOD and the *scid*. The *scid* (T and B – NOD), *scid* (T – NOD and B – IL4^{-/-}) showed a decrease in akt expression compared to the NOD and the *scid*. The *scid* (T - I μ ^{null} and B – IL4^{-/-}) decreased in akt expression compared to the *scid*, and remained stable compared to the NOD. The *scid* (B – IL4^{-/-}) depicted an increase in akt expression compared to the *scid* but remained stable compared to the NOD. The *scid* consistently had an increased level of akt expression from 4 weeks to 8 weeks, when compared to the NOD.

Table 3-5. Akt expression ratios.

Age of treated mouse	Akt expression ratio ^a (compared to NOD)	Akt expression ratio(compared to <i>scid</i>)	Akt expression ratio (<i>scid</i> compared to NOD)
4 wks – <i>scid</i> (Unfractionated NOD) (n = 4)	1X	>1X ^b	2X
>8 wks – <i>scid</i> (Unfractionated NOD) (n = 4)	2X	>1X	2X
4 wks – <i>scid</i> (T and B - NOD) (n = 4)	1X	1X	1X
>8 wks – <i>scid</i> (T and B - NOD) (n = 2)	>1X	>1X ^b	3X
4 wks – <i>scid</i> (T – NOD and B – IL4 ^{-/-}) (n = 4)	15X	2X	4X
>8 wks – <i>scid</i> (T – NOD and B – IL4 ^{-/-}) (n = 2)	4X	>1X ^b	5X
4 wks – <i>scid</i> (B – IL4 ^{-/-}) (n = 4)	2X	1X	3X
>8 wks – <i>scid</i> (B – IL4 ^{-/-}) (n = 4)	2X	2X	1X
4 wks – <i>scid</i> (T- I μ ^{null} and B – IL4 ^{-/-}) (n = 4)	2X	2X	2X
>8 wks – <i>scid</i> (T- I μ ^{null} and B – IL4 ^{-/-}) (n = 2)	2X	>1X ^b	4X
4 wks – <i>scid</i> (T- I μ ^{null}) (n = 4)	1X	2X	>1X
>8 wks – <i>scid</i> (T- I μ ^{null}) (n = 4)	NA	NA	NA
4 wks – <i>scid</i> (T- I μ ^{null} and B – NOD) (n = 4)	NA	NA	NA
>8 wks – <i>scid</i> (T- I μ ^{null} and B – NOD) (n = 3)	1X	2X	1X

^aThe fold increase ratio based on the akt expression detected by gel electrophoresis.

^bThe amount of akt expressed is 2x or more than the *scid* control when compared to the adoptively-transferred *scid*.

In Situ Apoptosis Detection Kit.

The presence of apoptotic cells was detected by TUNEL staining using fixed section of smg. As seen in Fig. 3-3, apoptosis has detected in untreated *scid* mice at 4 wks post-transfer and 8 wks post-transfer. Apoptotic cells were also detected in the *scid* (T and B - NOD) mouse, *scid* (T - I μ^{null} and B - IL-4^{-/-}) mouse and the *scid* (T - I μ^{null} and B - NOD) mouse. The average number of apoptotic cells per five fields was determined. As seen in Table 3-6, the adoptively transferred *scid* mice showed a higher number of apoptotic cells compared to the *scid* parental controls.

Detection of Infiltration

Immunohistochemistry

Many classification systems use the presence of infiltration in the salivary glands as a definitive marker of SjS. Lymphocytic infiltrates are seen in patients with SjS and the NOD/LtJ. After euthanization the submandibular glands of the adoptively-transferred and control mice were removed. A fraction of those submandibular glands were fixed and set in paraffin blocks. Afterwards, sections of paraffinized tissue were placed onto glass slides. The tissue was then treated with immunohistochemistry reagents to visualize infiltrates present in the submandibular gland. These slides were stained with Vector Red™ and DAB to visualize T and B-cells, respectively. A stained T-cell appears red and the B-cell appears as brown. A light green counterstain was used as well. As seen in Figs. 3-3 A and 3-3 A, there is no infiltrates present in the NOD-*scid*. Figs. 3-3 B and 3-3 B show infiltration of NOD/LtJ submandibular glands. There is a predominance of B-cells in the population. Figs. 3-3 C and 3-3 C show infiltration is present in the *scid* (T - I μ^{null} + B - IL4^{-/-}), with T-cells being the predominate cell.

Sections of paraffinized tissue were also made into hematoxylin and eosin stained slide. The slides were visualized by brightfield microscopy in order to detect the presence of infiltrates. Infiltrated lymphocytes were counted to determine the focus score. The NOD at both 4 weeks and 8 weeks post-transfer had a focus score of >2 (Table 3-6). The *scid* positive control did not show any infiltration at week 4 or week 8.

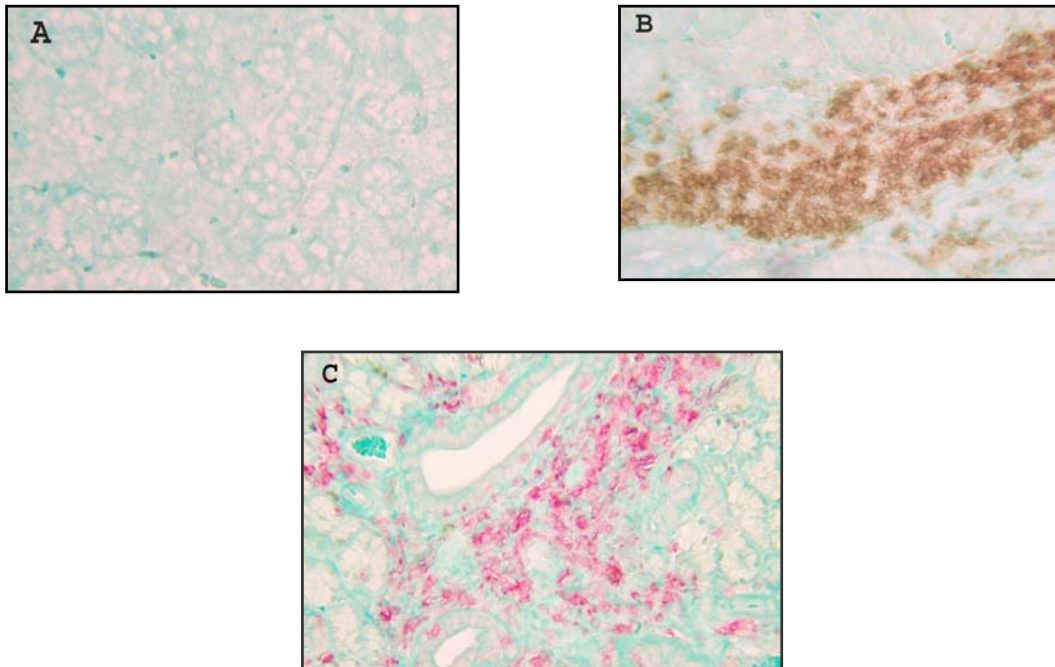


Figure 3-2: Immunohistochemical staining of submandibular glands for lymphocyte-infiltrations. Staining was performed on paraffin-embedded sections of submandibular glands. B-cells stained with DAB (brown), T-cells stained with VectorRed (red) and counterstained with light green. A) 20 wk old NOD-*scid* smg gland; focus score = 0. B) 20 wk old NOD/LtJ smg gland; focus score = 1. C) 16 wk old (4 wks post-transfer) NOD-*scid* (T - $Ig\mu^{null}$ + B - $IL4^{-/-}$); focus score = 1. Magnification = 10x.

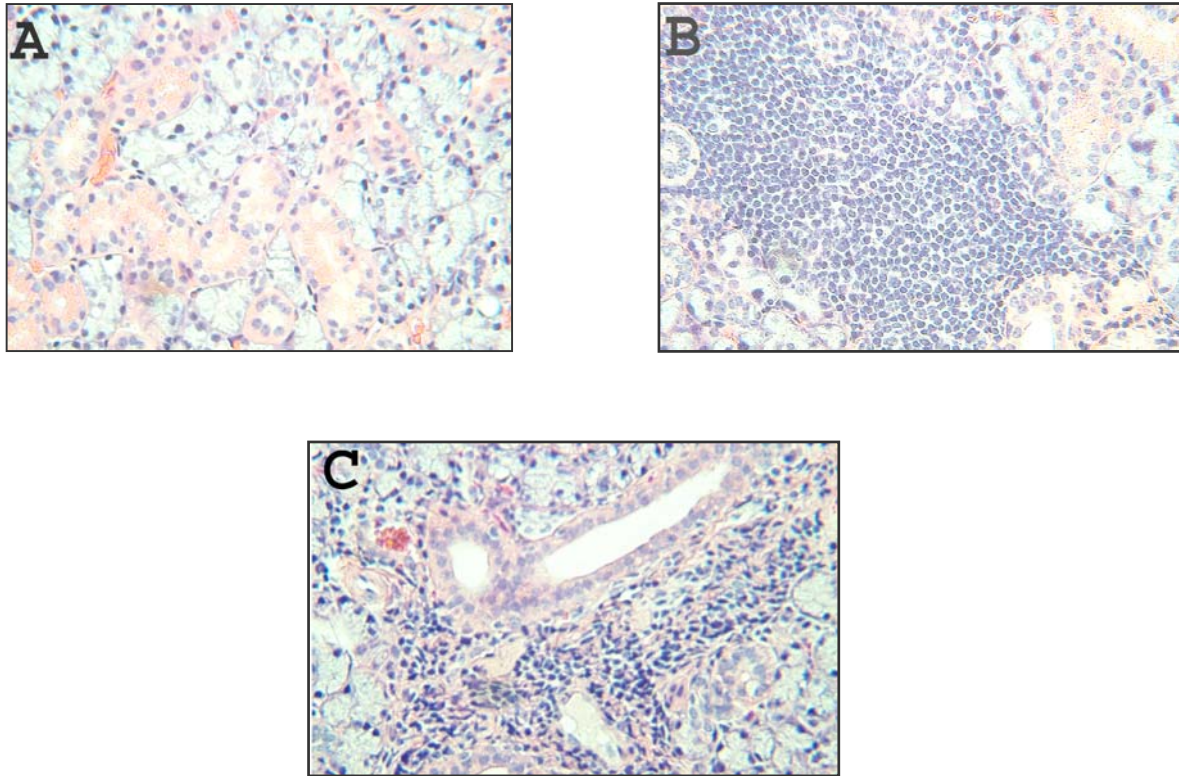


Figure 3-3. Hematoxylin/eosin-stained tissue sections of submandibular glands. Staining was performed on paraffin-embedded sections of submandibular glands. A) 20 wk old NOD-*scid* smg gland; focus score = 0. B) 20 wk old NOD/LtJ smg gland; focus score = 1. C) 16 wk old (4 wks post-transfer) NOD-*scid* (T - I μ^{null} + B - IL4^{-/-}); focus score = 1. Magnification = 10x.

The *scid* (T and B - NOD) had a focus score of >2 at 4 weeks with no infiltration seen by week 8. The *scid* (T - I μ^{null} and B - IL4^{-/-}) at 4 weeks post transfer had a focus score of 1 (moderate infiltration), but by 8 weeks no infiltration was detected. The *scid* (T - I μ^{null} and B - NOD) showed no infiltration at 4 weeks with a focus score of >2 at 8 weeks. The other adoptively transferred mouse groups did not show infiltration at 4 weeks or 8 weeks post-transfer.

Table 3-6. Focus score derived from H+E stained slides of smg glands. A focus score of 1 is equivalent to 50 lymphocytes in a view. 50 lymphocytes in a view is given a score of 1; 100 lymphocytes is given a score of 2; and over 100 lymphocytes is given a score of >2.

Recipient NOD- <i>scid</i> (age)	Donor cells	Focus score
NOD/LtJ 4 weeks	Positive Control	>2
8 weeks		>2
NOD- <i>scid</i> 4 weeks	Negative Control	0
8 weeks		0
NOD- <i>scid</i> 4 weeks	Unfractionated NOD	0
8 weeks	Unfractionated NOD	0
NOD- <i>scid</i> 4 weeks	T and B - NOD	>2
8 weeks	T and B - NOD	0
NOD- <i>scid</i> 4 weeks	T- NOD and B- IL4 ^{-/-}	0
8 weeks	T- NOD and B- IL4 ^{-/-}	0
NOD- <i>scid</i> 4 weeks	B - IL4 ^{-/-}	0
8 weeks	B - IL4 ^{-/-}	0
NOD- <i>scid</i> 4 weeks	T- Igμ ^{null} and B - IL4 ^{-/-}	1
8 weeks	T- Igμ ^{null} and B- IL4 ^{-/-}	0
NOD- <i>scid</i> 4 weeks	T - Igμ ^{null}	0
8 weeks	T - Igμ ^{null}	0
NOD- <i>scid</i> 4 weeks	T - Igμ ^{null} and B - NOD	0
8 weeks	T - Igμ ^{null} and B - NOD	>2

CHAPTER 4 DISCUSSION

Studies using the NOD-*scid* mouse have led to advancement in the research of SjS. Observations on the *scid* mouse have provided clarification of the glandular and protein changes that occur in the salivary gland in phase I of SjS disease. Although the *scid* mouse has these glandular changes, its lack of progression to phase II identifies the critical role lymphocytes have in development of phase II of the disease. Providing the *scid* mouse with appropriate lymphocytes was hypothesized to result in progression of phase II. The results of this thesis provide details on the ability to adoptively transfer various combinations of lymphocytes from the NOD/LtJ, NOD.IL-4^{-/-}, and NOD.Igμ^{null} into the NOD-*scid* mouse, thereby, transferring phase II of SjS to this non-autoimmune host.

The NOD mouse is considered a good mouse model for SjS research and is the positive control used in the research of this thesis. It is expected that lymphocytes from the NOD, placed in the *scid* mouse, should result in SjS development. The data show a 46% decrease in the salivary flow, of adoptively transferred *scid* mice from week 4 post-transfer to week 8, receiving T and B-cells from the NOD. However, there is no change in the salivary flow of *scid* recipients of unfractionated NOD splenocytes. The stable salivary flow observed in the *scid* (Unfractionated NOD) mouse implies that there is a population of cells in the splenic lymphocytes capable of inhibiting disease transfer. The removal of this population allows for SjS progression, as seen in the

scid (T and B – NOD) mouse. Presumably, the T-cells from the NOD activates antibody production by the B – NOD, thus resulting in the observed salivary loss. The T – NOD also show an ability to transfer disease when combined with B-cells from the NOD.IL 4^{-/-}. The NOD.IL-4^{-/-} mouse does not develop phase II disease, even though disease precursors are present. The absence of IL - 4 cytokine, which is necessary for class switching, prevents disease progression. However, T-cells from NOD mice provide the IL-4 cytokine, thus allowing antibody production and the resulting decrease in salivation. The *scid* (B – IL-4^{-/-}) mouse had little change in saliva volume, possibly due to the absence of an appropriate T-cell. B –cells from the NOD mouse, as seen in the *scid* (T and B – NOD) mouse, have an ability to transfer disease when activated by an appropriate T-cell. The NOD.Igμ^{null}, which lacks B-cells, has functional T-cells that produce IL-4 and are capable of activating B-cells. The recipients of T-cells from the Igμ^{null} mouse and B-cells from the NOD mouse did not show a decrease in salivary flow as might be predicted, yet transfer of phase II is possible as shown by the *scid* (T and B - NOD) mouse and the *scid* (T - NOD and B - IL-4^{-/-}) mouse. Thus, transferred disease may be delayed in certain combinations, such as the *scid* (T - Igμ^{null} and B – NOD) mouse. In the NOD environment, antigen presentation by B-cells to T-cells, or other APC, may occur before the splenocytes are fractionated. Under such conditions, T-cells are already producing the cytokines required for class switching before transfer into the *scid* mouse. This would allow for rapid transfer of disease. However the Igμ^{null}, without B-cells capable of presenting antigens, may have “naïve” T-cells. Transfer of these “naïve” T-cells may then require a longer incubation for development of phase II. Thus, it is possible that *scid* recipients of T – Igμ^{null} and

B – IL-4^{-/-} did not show a decrease in salivary flow at 8 weeks post-transfer due to the “naïve” nature T-cells from the I μ ^{null} mouse. In a previous study, T-cells from the I μ ^{null} were transferred into the IL-4^{-/-} mouse, resulting in development of phase II (23). However, the researchers of this study allotted more incubation time for progression of phase II (12 weeks compared to the 8 weeks allotted in this thesis). It is also possible that there is a loss in salivary flow in the *scid* (T - I μ ^{null} and B – NOD) mouse and the *scid* (T - I μ ^{null} and B – IL-4^{-/-}), but this loss is belied by the method of collection. Pooling of saliva during collection and then quantifying may mask any loss of salivary flow that is occurring in some of the treated mice. In the *scid* (T and B – NOD) mouse and the *scid* (T – NOD and B – IL-4^{-/-}) mouse the loss of salivary flow for the 4 *scid* mice was not simultaneous. A variation in timing of the appearance of phase II was also observed in the T - I μ ^{null} transfer to NOD.IL-4^{-/-} study. The *scid* recipients of T-cells from the I μ ^{null} mouse had normal salivary flow, indicating no disease progression.

The NOD has been shown previously to be a good positive control, typically having a 45 - 75% loss in salivary flow by 20 weeks of age (17,22,25). However, a loss in saliva volume was not detected in these experiments. Nevertheless, the parental NOD-*scid* mouse had stable salivary flow. Diabetes, a disease present in the NOD, appeared in all of the *scid* mice that received B and T-cells from the NOD, but not unfractionated splenocytes. It is apparent that diabetes was co-transferred with phase II. Due to the presence of diabetes, 0.1 cc of insulin was administered to each mouse, once a day. Despite treatment, a few of the experimental and positive controls expired early. In order

to prevent the loss of all of the treated mice, some were euthanized prior to 8 weeks post transfer. This early euthanization could have affected the results.

Concomitant with the loss of saliva secretion, there are significant changes in the composition and activity of salivary proteins. Probably indicating multiple mechanisms of action. The decline in amylase may be a result of glandular changes that results from defects in glandular homeostasis (21). Amylase, an enzyme that hydrolyzes starch, is one of the glandular proteins that have an age-related decline in NOD and *scid* mice, and therefore, a marker of phase I disease. The NOD and *scid* controls, as well as the adoptively transferred *scid* mice, all had a decline in salivary amylase activity with the exception of the *scid* (Unfractionated NOD) mouse and *scid* (T – NOD and B – IL-4^{-/-}) mouse, which had increases of 46%. The decline in amylase activity indicates that there are glandular changes occurring, to which the adoptively transferred lymphocytes may respond. Although the *scid* (T – NOD and B – IL-4^{-/-}) mouse has an increase in amylase activity, the decrease in salivary flow suggests transfer of disease. It is not clear why there is a discrepancy in this particular adoptive transfer combination. Observation of the results shows variability in the amylase activity of the submandibular glands amongst the treated *scid* mice. The NOD positive control and *scid* negative control both showed a decline in amylase activity in the submandibular gland lysate. The *scid* (T and B – NOD) mouse, *scid* (T – I μ ^{null} and B – IL-4^{-/-}) mouse and *scid* (T – I μ ^{null} and B – NOD) mouse showed variable levels of declining amylase activity in the submandibular gland. However, the *scid* (Unfractionated NOD) mouse, *scid* (T – NOD and B – IL-4^{-/-}) mouse, *scid* (B – IL-4^{-/-}) mouse and *scid* (T - I μ ^{null}) mouse showed an increase in amylase activity. It is not certain what causes such variability in detection of amylase activity in

the submandibular gland, when this same method is useful for detection of salivary amylase activity. There seemed to be significantly less amylase in the submandibular gland lysate compared to the saliva. Many samples were analyzed undiluted (a few were diluted 1:100). From a technical point of view, though, it is possible that this assay was not sensitive enough to detect amylase activity in the smg lysate.

Phase I of SjS is marked by aberrant production of salivary proteins. There is production of two neoteric forms of PSP, which enables the protein concentration to remain constant, despite declines in other major proteins (21). Results show that there is no change in salivary protein concentration for the adoptively transferred mice or the controls. However, there were decreases in submandibular gland lysate protein concentration from *scid* mice that received a combination of T and B-cells, irrespective of the origin of the lymphocytes. These decreases in protein concentration from 4 weeks to 8 weeks post-transfer may be indicative of degradation of the submandibular gland by apoptosis. The *scid* (T - I μ ^{null}) mouse also exhibited a decrease in protein concentration.

Apoptosis was measured to determine the effect the transferred lymphocytes may have on inducing cell death in the submandibular gland. Apoptosis occurs in the NOD and the *scid* during phase I of SjS. This apoptosis is lymphocyte-independent and is most likely a result of the aberrant glandular homeostasis (27,28,29). As SjS progresses to the effector stage, the NOD mouse exhibits increased levels of apoptosis in the submandibular gland, which has been shown to be lymphocyte-dependent (13). The results of the caspase-3 activity analysis revealed an increase of activity in all of the *scid* recipients receiving combinations of T and B-cells, except for the

scid (Unfractionated NOD) mouse. The increase in Caspase-3 activity in *scid* recipients of T and B-cell transfer, indicate that the transferred lymphocytes have an effect on apoptosis. The *scid* (T – I μ^{null}) mouse had a large increase (120%) in caspase activity. This may indicate that there is T-cell dependent role in apoptosis via cytokine production or cytotoxic action of CD8⁺ T-cells.

Caspase-3 activation is one of the last required events before apoptosis is completed, thus the observed increase in activity. However, AKT, as an inhibitor of apoptosis, would exhibit a decrease of expression. The results indicate a decrease in AKT expression in the *scid* (T and B – NOD) mouse and *scid* (T – NOD and B – IL-4^{-/-}) mouse compared to the level of AKT expression in the NOD. These groups also had a decrease of AKT expression when compared to the *scid* negative control. These findings suggest that AKT production has been decreased and may be allowing activation of apoptosis in the submandibular gland. This correlates with the increased level of caspase-3 activity seen in these two groups. Interestingly, the *scid* (Unfractionated NOD) mouse depicted an increase of AKT expression when compared to the NOD and *scid*, as well as a decrease in caspase-3 activity. This is possibly due to what is still an unidentified, inhibitory factor in the unfractionated NOD splenocyte population. The *scid* (B – IL-4^{-/-}) mouse did not show a decrease in AKT expression when compared to the NOD mouse and had a slight increase in expression, when compared to the *scid* mouse. The increase of AKT expression in the *scid* (B – IL-4^{-/-}) mouse and concurrent decrease of caspase-3 activity, would indicate a cessation in apoptosis activity. The *scid* (T – I μ^{null} and B – IL-4^{-/-}) mouse did not show a decrease in AKT expression compared to the NOD, but had a decrease in AKT expression compared to the *scid*

mouse. This group also showed an increased level of caspase-3 activity, which is indicative of apoptosis. The *scid* positive control had an average 2-fold increase of AKT expression compared to the NOD mouse.

The presence of elevated caspase-3 activity and decreased AKT expression suggests the presence of apoptotic cells. Visualization of apoptotic cells by flow cytometry was attempted. However, apoptosis was only detected in the *scid* (T – I μ^{null}) mouse and *scid* (B – IL-4^{-/-}) mouse. It is possible that apoptotic cells were lost in the preparation of the acinar cells and unable to be detected by flow cytometry. The high level of apoptosis detected in the *scid* (T - I μ^{null}) mouse by flow cytometry may be the result of cytokine production. It is not clear why a high level of apoptosis was detectable in the *scid* (B – IL-4^{-/-}) mouse. The results of the TUNEL stain show apoptotic cells in the *scid* mouse, parental control and the adoptively treated *scid* mice. Previous studies show that apoptotic cells are present in phase II, thereby indicating the development of phase II in the adoptively transferred *scid* mice. Previous findings show that the number of apoptotic cells increases as the *scid* mouse ages (17,19). However the NOD-*scid* parental control had a decrease in the number of apoptotic cells present.

A definitive aspect of SjS is the appearance of infiltrates in the submandibular gland. The results from the stained histology slides show the presence of infiltrating lymphocytes in the *scid* (T and B - NOD) mouse, *scid* (T – I μ^{null} and B – IL-4^{-/-}) mouse, and the *scid* (T – I μ^{null} and B – IL-4^{-/-}) mouse. This localization of lymphocytes in the submandibular gland is a precursor to the loss of salivary flow, thus indicating a transfer of SjS-like disease. Interestingly, the *scid* (T and B – NOD) mouse depict a high level of infiltration (focus score >2) at 4 weeks, and also exhibited a decrease in salivation.

However, the *scid* (T - I μ^{null} and B – NOD) mouse did not have infiltration until 8 weeks post-transfer, and did not lose salivary flow within that time. This supports the theory that adoptive transfer of T-cells from the I μ^{null} mouse into the *scid* recipient may require a longer incubation for SjS to develop. A similar situation is observed in the *scid* (T - I μ^{null} and B – IL-4 $^{-/-}$) mouse, which had a lesser amount of infiltration than the *scid* (T and B – NOD) mouse and did not have a decrease in salivation at 8 weeks post-transfer. Infiltration in the *scid* (T – NOD and B – IL-4 $^{-/-}$) mouse was not observed at 4 or 8 weeks post-transfer; however, there was a loss of salivary flow. This raises the possibility of a great effect by cytokine or other soluble factors.

In conclusion, transfer of a clinical Sjögren's Syndrome-like disease into the *scid* mouse by adoptive transfer is possible under certain conditions. The results of this thesis show that a transfer of T-cells from the NOD with functional B-cells will allow transfer of phase II to the *scid* recipient. Seemingly, the transfer of entire NOD splenocyte population may allow for a delay in SjS or even disease prevention. The results of the different analysis show that the *scid* (Unfractionated NOD) mouse consistently had results that were contradictory to the results observed in the *scid* (T and B – NOD) mouse. This provides more evidence of a possible inhibitory factor present in the unfractionated NOD splenocytes. There is a population of T-cells that can inhibit development of diabetes suggesting an important role of regulatory cells within the NOD mouse. This population may be present in the unfractionated population, and capable of preventing disease progression. Although the loss of salivary flow was not detected in adoptive transfer of T-cells from the I μ^{null} mouse together with functional B-cells, adoptive transfer of phase II may be possible. It is possible that T-cells from the I μ^{null}

may not be presented with the necessary antigens until interacting with a functional B-cell. In this situation, the development of disease would require a longer period of time. It is also probable that pooling of saliva during collection may mask individual changes in flow rates and protein content, especially since the loss of salivation may occur at different times in individual mice. Future directions of this research would be to use the NOD.B10.H-2^b mouse as one of the donor mice. The NOD.B10.H-2^b develops SjS, but does not develop diabetes as per the NOD (30), thus preventing diabetes complications. Utilization of the NOD.B10.H-2^b should allow for longer observation of the treated *scid* mice. In addition to the analysis performed in this study, detection of autoantibodies in the adoptively transferred mouse sera would be beneficial. Completion of future experiments may lead to a clarification of the etiopathology of Sjögren's Syndrome, which may result in better treatment for human patients.

LIST OF REFERENCES

1. Vivino F. The treatment of Sjögren's syndrome patients with Pilocarpine-tablets. *Scand J Rheumatol* 2001;115:1-13.
2. Jonsson R, Moen K, Vestrheim D, Szodoray P. Current issues in Sjögren's syndrome. *Oral Diseases* 2002;8:130-140.
3. Nepom GT. MHC and autoimmune diseases. *Immunol Ser.* 1993;59:143-64.
4. Davidson BK, Kelly CA, Griffiths ID. Primary Sjogren's syndrome in the North East of England: a long-term follow-up study. *Rheumatology (Oxford)*. 1999 Mar;38(3):245-53.
5. Rolando M. Sjogren's syndrome as seen by an ophthalmologist. *Scand J Rheumatol Suppl.* 2001;(115):27-31; discussion 31-3.
6. Harley JB, Alexander EL, Bias WB, Fox OF, Provost TT, Reichlin M, Yamagata H, Arnett FC. Anti-Ro (SS-A) and anti-La (SS-B) in patients with Sjogren's syndrome. *Arthritis Rheum.* 1986 Feb;29(2):196-206.
7. Kelly CA, Foster H, Pal B, Gardiner P, Malcolm AJ, Charles P, Blair GS, Howe J, Dick WC, Griffiths ID. Primary Sjogren's syndrome in north east England--a longitudinal study. *Br J Rheumatol.* 1991 Dec;30(6):437-42.
8. Reveille JD. The molecular genetics of systemic lupus erythematosus and Sjogren's syndrome. *Curr Opin Rheumatol.* 1992 Oct;4(5):644-56.
9. The Jackson Laboratory. <http://jaxmice.jax.org/jaxmice-cgi/jaxmicedb.cgi?objtype=pricedetail&stock=001976> (Accessed 24 March 2003).
10. Humphreys-Beher MG, Brinkley L, Purushotham KR, Wang PL, Nakagawa Y, Dusek D, Kerr M, Chegini N, Chan EK. Characterization of antinuclear autoantibodies present in the serum from nonobese diabetic (NOD) mice. *Clin Immunol Immunopathol.* 1993 Sep;68(3):350-6.
11. van Blokland SC, Versnel MA. Pathogenesis of Sjogren's syndrome: characteristics of different mouse models for autoimmune exocrinopathy. *Clin Immunol.* 2002 May;103(2):111-24.

12. Humphreys-Beher MG, Yamachika S, Yamamoto H, Maeda N, Nakagawa Y, Peck AB, Robinson CP. Salivary gland changes in the NOD mouse model for Sjogren's syndrome: is there a non-immune genetic trigger? *Eur J Morphol*. 1998 Aug;36 Suppl:247-51.
13. van Blokland SC, van Helden-Meeuwssen CG, Wierenga-Wolf AF, Drexhage HA, Hooijkaas H, van de Merwe JP, Versnel MA. Two different types of sialoadenitis in the NOD- and MRL/lpr mouse models for Sjogren's syndrome: a differential role for dendritic cells in the initiation of sialoadenitis? *Lab Invest*. 2000 Apr;80(4):575-85.
14. Stott DI, Hiepe F, Hummel M, Steinhauser G, Berek C. Antigen-driven clonal proliferation of B-cells within the target tissue of an autoimmune disease. The salivary glands of patients with Sjogren's syndrome. *J Clin Invest*. 1998 Sep 1;102(5):938-46.
15. Crispin JC, Vargas MI, Alcocer-Varela J. Immunoregulatory T-cells in autoimmunity. *Autoimmun Rev*. 2004 Feb;3(2):45-51.
16. Rudin CM and Thompson CB. Apoptosis and disease; Regulation and clinical relevance of programmed cell death. *Annu Rev Med*. 1997;48:267-81.
17. Kong L, Robinson CP, Peck AB, Vela-Roch N, Sakata KM, Dang H, Talal N, Humphreys-Beher MG. Inappropriate apoptosis of salivary and lacrimal gland epithelium of immunodeficient NOD-*scid* mice. *Clin Exp Rheumatol*. 1998 Nov-Dec;16(6):675-81.
18. Goillot E, Mutin M, Touraine JL. Sialadenitis in nonobese diabetic mice: transfer into syngeneic healthy neonates by splenic T lymphocytes. *Clin Immunol Immunopathol*. 1991 Jun;59(3):462-73.
19. Bacman S, Sterin-Borda L, Camusso JJ, Arana R, Hubscher O, Borda E. Circulating antibodies against rat parotid gland M3 muscarinic receptors in primary Sjogren's syndrome. *Clin Exp Immunol*. 1996 Jun;104(3):454-9.
20. Nguyen KH, Brayer J, Cha S, Diggs S, Yasunari U, Hilal G, Peck AB, Humphreys-Beher MG. Evidence for antimuscarinic acetylcholine receptor antibody-mediated secretory dysfunction in nod mice. *Arthritis Rheum*. 2000 Oct;43(10):2297-306.
21. Robinson CP, Yamamoto H, Peck AB, Humphreys-Beher MG. Genetically programmed development of salivary gland abnormalities in the NOD (nonobese diabetic)-*scid* mouse in the absence of detectable lymphocytic infiltration: a potential trigger for sialoadenitis of NOD mice. *Clin Immunol Immunopathol*. 1996 Apr;79(1):50-9.

22. Robinson CP, Brayer J, Yamachika S, Esch TR, Peck AB, Stewart CA, Peen E, Jonsson R, Humphreys-Beher MG. Transfer of human serum IgG to nonobese diabetic Igm null mice reveals a role for autoantibodies in the loss of secretory function of exocrine tissues in Sjogren's syndrome. *Proc Natl Acad Sci U S A*. 1998 Jun 23;95(13):7538-43.
23. Brayer JB, Cha S, Nagashima H, Yasunari U, Lindberg A, Diggs S, Martinez J, Goa J, Humphreys-Beher MG, Peck AB. IL-4-dependent effector phase in autoimmune exocrinopathy as defined by the NOD.IL-4-gene knockout mouse model of Sjogren's syndrome. *Scand J Immunol*. 2001 Jul-Aug;54(1-2):133-40.
24. Rohane PW, Shimada A, Kim DT, Edwards CT, Charlton B, Shultz LD, Fathman CG. Islet-infiltrating lymphocytes from prediabetic NOD mice rapidly transfer diabetes to NOD-*scid/scid* mice. *Diabetes*. 1995 May;44(5):550-4.
25. Szanya V, Ermann J, Taylor C, Holness C, Fathman CG. The subpopulation of CD4+CD25+ splenocytes that delays adoptive transfer of diabetes expresses L-selectin and high levels of CCR7. *J Immunol*. 2002 Sep 1;169(5):2461-5.
26. Serreze DV, Chapman HD, Varnum DS, Hanson MS, Reifsnnyder PC, Richard SD, Fleming SA, Leiter EH, Shultz LD. B lymphocytes are essential for the initiation of T cell-mediated autoimmune diabetes: analysis of a new "speed congenic" stock of NOD.Ig mu null mice. *J Exp Med*. 1996 Nov 1;184(5):2049-53.
27. van Blokland SC, Van Helden-Meeuwsen CG, Wierenga-Wolf AF, Tielemans D, Drexhage HA, Van De Merwe JP, Homo-Delarche F, Versnel MA. Apoptosis and apoptosis-related molecules in the submandibular gland of the nonobese diabetic mouse model for Sjogren's syndrome: limited role for apoptosis in the development of sialoadenitis. *Lab Invest*. 2003 Jan;83(1):3-11.
28. Humphreys-Beher MG, Peck AB, Dang H, Talal N. The role of apoptosis in the initiation of the autoimmune response in Sjögren's Syndrome. *Clin Exp Immunol*. 1999 Jan; 116: 383-387.
29. Yamamoto H, Sims NE, Macauley SP, Nguyen KH, Nakagawa Y, Humphreys-Beher MG. Alterations in the secretory response of non-obese diabetic (NOD) mice to muscarinic receptor stimulation. *Clin Immunol Immunopathol*. 1996 Mar;78(3):245-55.
30. Cha S, van Blockland SC, Versnel MA, Homo-Delarche F, Nagashima H, Brayer J, Peck AB, Humphreys-Beher MG. Abnormal organogenesis in salivary gland development may initiate adult onset of autoimmune exocrinopathy. *Exp Clin Immunogenet*. 2001;18(3):143-60.

BIOGRAPHICAL SKETCH

Vinette B. Brown was born in Brooklyn, New York, in 1979. She comes from a very large extended Jamaican family. When she was 10 years old, she and her parents moved to Hollywood, Florida, where she graduated from Hollywood Hills High School in 1997. Afterwards, she received a Bachelor of Science in zoology, with a minor in business from the University of Florida in 2001. She went on to receive a Master of Science in molecular genetics and microbiology in August 2004 from the University of Florida. Vinette will work towards earning a Doctor of Dental Science degree at the School of Dental and Oral Surgery at Columbia University.